Human Tau aggregates are permissive to Protein Synthesis Dependent Memory in Drosophila Tauopathy models

Ergina Vourkou[1], Eva D. Rouiz Ortega[2], Sumeet Mahajan[3], Amrit Mudher[2] and Efthimios MC Skoulakis[1*]

[1]Institute for Fundamental Biomedical Research, Biomedical Sciences Research Centre "Alexander Fleming", Vari 16672 Greece

[2]School of Biological Sciences, Faculty of Environmental and Life Sciences, University of Southampton, Highfield Southampton SO17 1BJ UK

[3]School of Chemistry, Institute for Life Sciences, University of Southampton, Highfield Southampton SO17 1BJ UK

[*]correspondence to EMC Skoulakis: skoulakis@fleming.gr

Running title: Tau aggregates facilitate neuroplasticity

Keywords: Tau, Tau aggregation, Memory, Methylene Blue, Drosophila

ABSTRACT

Tauopathies including Alzheimer's disease, are characterized by progressive cognitive decline, neurodegeneration and intraneuronal aggregates comprised largely of the axonal protein Tau. It has been unclear whether cognitive deficits are consequent of aggregate accumulation which compromise neuronal health and eventually lead to neurodegeneration. We use the Drosophila Tauopathy model and mixed sex populations to reveal an adult onset pan-neuronal Tau accumulation-dependent decline in learning efficacy and a specific defect in Protein Synthesis Dependent Memory (PSD-M), but not in its Protein Synthesis Independent variant. We demonstrate that these neuroplasticity defects are reversible upon suppression of new transgenic human Tau expression, but surprisingly correlate with an increase in Tau aggregates. Inhibition of aggregate formation via acute oral administration of Methylene Blue results in re-emergence of deficient memory in animals with suppressed $hTau^{0N4R}$ expression. Significantly, aggregate inhibition results in PSD-M deficits in $hTau^{0N3R}$-expressing animals, which present elevated aggregates and normal memory if untreated with Methylene Blue. Moreover, Methylene Blue-dependent $hTau^{0N4R}$ aggregate suppression within adult mushroom body neurons, also resulted in emergence of memory deficits. Therefore, deficient PSD-M upon human Tau expression in the Drosophila CNS is not consequent of toxicity and neuronal loss because it is reversible. Furthermore, PSD-M deficits do not result from aggregate accumulation, which appears permissive, if not protective of processes underlying this memory variant.

SIGNIFICANCE STATEMENT

Intraneuronal Tau aggregate accumulation has been proposed to underlie the cognitive decline and eventual neurotoxicity that characterizes the neurodegenerative dementias known as Tauopathies. However, we show in three experimental settings that Tau aggregates in the Drosophila CNS do not impair, but rather appear to facilitate processes underlying Protein Synthesis Dependent memory within affected neurons.

INTRODUCTION

Tauopathies, involve dysregulation of the essential neuronal microtubule (MT)-associated protein Tau and are the most widespread neurodegenerative dementias including Alzheimer's (AD) and Pick's (PiD) diseases among others (Spillantini and Goedert 1998, Lee *et al.* 2001, Delacourte 2005, Zhang *et al.* 2022). There are 6 Tau isoforms in the human Central Nervous System (CNS) arising by alternative splicing of a single transcript (Andreadis *et al.* 1995, Arendt *et al.* 2016, Zhang *et al.* 2022) and are engaged in multiple intraneuronal processes including axonal microtubule stability and function (Wang and Mandelkow 2015, Sotiropoulos *et al.* 2017).

Although the initiating mechanisms remain largely elusive, pathogenic transformation of physiological Tau isoforms is characterized by their hyper-phosphorylation and eventual aggregate formation (Alonso *et al.* 2001, Cowan and Mudher 2013, Arendt *et al.* 2016). This has led to hypotheses positing that aggregates act as "gain of function" mutations (Trojanowski and Lee 2005), obstructing housekeeping or neuroplasticity mechanisms and mediate neuronal dysfunction, toxicity and neurodegeneration (Wang and Mandelkow 2015, Arendt *et al.* 2016, Zhang *et al.* 2022). However, the contribution of aggregates, such as the characteristic Neurofibrillary tangles (NFTs) in neuronal dysfunction and neurodegeneration has been questioned (Spires-Jones *et al.* 2009, Spires-Jones *et al.* 2011, Wang and Mandelkow 2015). Typically, NFT formation is preceded by cognitive deficits (Andorfer *et al.* 2005) and their presence generally does not correlate with cognitive deficits in mouse Tauopathy models (Santacruz *et al.* 2005, Sydow *et al.* 2011, Van der Jeugd *et al.* 2012). In Drosophila, pharmacological, or genetic inhibition of hyper-phosphorylation which reverses Tau mediated dysfunction is reported to be accompanied by increased Tau aggregation (Cowan *et al.* 2015). Furthermore, inhibition of Tau aggregation in clinical trials did not benefit AD patients or ones with the behavioural variant of Frontotemporal Dementia (Wischik *et al.* 1996, Wischik *et al.* 2015, Gauthier *et al.* 2016, Shiells *et al.* 2020). Therefore, though larger Tau aggregates such NFTs may eventually mediate neuronal death and underlie neurodegeneration, they appear unlikely to be causal of neuronal dysfunction and initial cognitive deficits.

Tau is proposed to form extended β-sheet amyloid-like filamentous inclusions with structures characterizing distinct Tauopathies (Shi *et al.* 2021), via a stepwise mechanism involving a number of apparent intermediates. Pathologically hyper-phosphorylated Tau is thought to form oligomers such as dimers and trimers, which act as intermediates and promote formation of larger globular oligomers, which aggregate further adopting β-sheet conformations, to yield filaments and eventually NFTs (Sahara *et al.* 2007, Sahara *et al.* 2008, Patterson *et al.* 2011, Kaniyappan *et al.* 2017). Small oligomers, comprised of few to a dozen monomers are thought to be soluble, while larger insoluble ones are referred to as granular oligomers or GTOs (Cowan *et al.* 2015). Significantly, the small oligomers have

been linked to neuronal dysfunction and synaptotoxicity (Kaniyappan *et al.* 2017), whilst the larger ones form in conditions associated with suppression of these phenotypes (Cowan *et al.* 2015).

We aimed to determine whether Tau aggregation underlies cognitive deficits capitalizing on the genetic facility of a Drosophila Tauopathy model (Papanikolopoulou and Skoulakis 2011, Giong *et al.* 2021). Human Tau isoform-encoding transgenes expressed in the adult Drosophila CNS result in isoform and time-dependent deficits in associative learning (Mershin *et al.* 2004, Kosmidis *et al.* 2010, Papanikolopoulou and Skoulakis 2015, Sealey *et al.* 2017, Keramidis *et al.* 2020) and memory (Prifti *et al.* 2022). The exquisite spatiotemporal regulation of transgene expression in this system (McGuire *et al.* 2004, McGuire *et al.* 2004), affords precise description of Tau pathogenic modifications ostensibly underlying learning deficits (Papanikolopoulou and Skoulakis 2015) and the formation of high molecular weight aggregates (Cowan and Mudher 2013, Papanikolopoulou and Skoulakis 2015, Sealey *et al.* 2017). Utilizing regulated spatiotemporal expression in the fly CNS of two human Tau isoforms, one known to precipitate learning defects and another which does not (Sealey *et al.* 2017), we ask whether the presence of aggregates correlates with memory deficits.

MATERIALS AND METHODS

Drosophila culture and strains

Drosophila crosses were set up *en masse* in standard wheat-flour-sugar food supplemented with soy flour and $CaCl_2$ and cultured at 18°C and 50–70% humidity in a 12 h light/dark cycle unless noted otherwise. Adult-specific pan-neuronal and pan-mushroom body transgene expression was achieved using the $Elav^{C155}$-Gal4; Tub-$Gal80^{ts}$ (ElavGal4;$Gal80^{ts}$)(Papanikolopoulou and Skoulakis 2015) or LeoMB-Gal4; Tub-$Gal80^{ts}$ (LeoGal4;$Gal80^{ts}$) (Papanikolopoulou *et al.* 2019), respectively. The fly line carrying UAS-$htau^{0N4R}$ (0N4R) was a gift of Dr. M. Feany (Harvard Medical School, Boston, MA, United States) and UAS-$hTau^{0N3R}$ of Dr A. Mudher (University of Southampton). The generation of UAS-$hTau^{0N4Ra1}$ transgene has been described previously (Keramidis et al., 2020). The bacterial plasmid pGEX-5x expressing the $hTau^{0N4R}$ isoform was a kind gift from Dr. Martin Chow (University of Kentucky). The cDNA was subcloned into pUASattB vector (Bischof *et al.* 2007) as a BglII/XbaI fragment. The sequence of the construct was confirmed by dsDNA sequencing (VBC-biotech). Transgenic flies were generated by phiC31-mediated transgenesis by BestGene Inc. (Chino Hills, CA, USA). DNAs were injected into genomic landing site 53B2 and ZH-86Fb on the second ($0N4R^{a1}$) and third ($0N4R^{a2}$) chromosomes respectively (BDSC #9736 and BDSC#24749 respectively). The double Tau transgene strain ($0N4R^{2a}$) was constructed by standard genetic crosses of the above transgenes ($0N4R^{a1}$ and $0N4R^{a2}$). All initial fly strains were backcrossed into the resident Cantonized w^{1118} control background for six generations.

Drug feeding

Adult flies were collected and maintained on standard food supplement with Methylene Blue (MetBlu, Sigma) in the concentrations indicated in the text. Flies were transferred to fresh vials every 2 days.

Lifespan determination

Flies accumulating $hTau^{0N4R}$ or $hTau^{0N3R}$ under $Elav^{C155}$-Gal4; Tub-$Gal80^{ts}$ were raised at 18°C along with control driver heterozygotes. Groups of 20 young male flies (1-3 d old) were collected and maintained at the transgene-expression permissive temperature of 30°C until they expired. Flies were transferred to fresh vials every 3 days. For the drug experiments, flies were transferred to fresh food supplement with Methylene Blue every 2 days. At least 300 flies were assessed per genotype.

Behavioral analyses

Animals expressing UAS-$hTau^{0N4R}$ or UAS-$hTau^{0N3R}$ under the control of the $Elav^{C155}$-Gal4; Tub-$Gal80^{ts}$ or LeoMB-Gal4; Tub-$Gal80^{ts}$ drivers were raised at 18°C. Upon eclosion they were collected in fresh bottles or vials and transgene expression was induced by placing them at 30°C for 6 or 12 days. For expression reversal experiments, pan-neuronal transgene expression was allowed for 12 days at 30°C as before, but it was followed by 10 days of maintaining the flies at 18°C as described in the text and

flies were transferred to fresh vials with or without Methylene blue every 2 days. Flies on Methylene blue for behavioral testing were transferred to fresh vials without the drug for 1 h before conditioning commenced.

All associative learning and memory experiments were performed under dim red light, at 25°C and 70-75% humidity, in a genotype-balanced manner. All genotypes involved in an experiment were tested per day. Olfactory aversive conditioning was performed as previously described (Keramidis *et al.* 2020) using the aversive odors benzaldehyde (BNZ) and 3-octanol (OCT) diluted in isopropylmyristate (Fluka) (6% v/v for BNZ and 50% v/v for OCT) as conditioned stimuli (CS+ and CS−) with 90 Volt electric shocks as unconditioned stimuli (US). One hour before training flies were transferred to fresh food vials. To assess immediate memory (learning), a group of 50-70 flies were tested immediately after a single training cycle consisting of the CS + odor for 40 sec paired with eight 90V shocks, 30 sec air, and CS− odor for 40 sec without shock and then 30 sec of air. To assess immediate performance (learning) after 5-round *Extended Conditioning* (5X Immediate), flies were tested immediately after five training cycles each consisting of the CS + odor for 60 sec paired with 12 90V shocks, 30 sec air and CS− odor for 60 sec without shock and then 30 sec of air, with 15 min rest intervals between rounds. For 24-hr memory after *Spaced Conditioning* (PSD-M) flies were submitted to 12 US/CS pairings per round and five such training cycles with a 15 min rest interval between cycles as above, but they were kept at 18°C for 24 h before testing. For 24-hr memory after *Massed Conditioning* (PSI-M), flies were submitted to 12 US/CS pairings per round and five such rounds of training, without the 15 min inter-round interval. The flies were also kept at 18 °C until tested 24 hrs later. In all above experiments, two groups of animals of the same genotype were trained simultaneously with the CS+ and CS− odors switched. Both groups of flies were tested in a T-maze apparatus being allowed to choose between the two odors for 90 sec. A performance index (PI) was calculated as described before (Keramidis *et al.* 2020) and represents n=1.

RNA extraction and RT-PCR

Total RNA was extracted using Trizol Reagent (Sigma Millipore) following the manufacturer's instructions. Reverse transcription reaction was conducted using SuperScript II Reverse Transcriptase (Invitrogen) and 1µg cDNA from each RT reaction were then subjected to PCR using the following conditions: at 95°C for 10 min, followed by 28 cycles of 95°C for 60 sec, 62°C for 40 sec, and 72°C for 60 sec. A final extension step at 72^{o}C for 10min was performed and the PCR products were analyzed by agarose gel electrophoresis. The ribosomal gene rp49 was used as a normalizer. The primers used were: Tau-F:5′-CCCGCACCCCGTCCCTTCC-3′; Tau-R:5′-GATCTCCGCCCCGTGGTCTGTCTT-3′; rp49-F:5′-GATCGTGAAGAAGCGCAC-3′; and rp49-R: 5′-CTTCTTGAATCCGGTGGG-3′. Quantification was performed using the ImageJ software.

Western Blot and Antibodies

Total Tau levels in 3–6 adult female heads were determined by homogenization in 1x Laemmli buffer (50mM Tris, pH 6.8, 5% 2-mercaptoethanol, 2% SDS, 10% glycerol, and 0.01% bromophenol blue), boiling for 5 min at 95°C, centrifugation for 5 min at 11,000g and separation in 10% SDS-acrylamide gels. Proteins were transferred to PVDF membranes and probed with mouse monoclonal anti-Tau (5A6, Developmental Studies Hybridoma Bank) at a 1:1,000 dilution. Anti-syntaxin (Syx) primary antibody (8C3, Developmental Studies Hybridoma Bank) at a 1:3,000 was used to normalize sample loading. HRP-conjugated secondary antibodies were applied at 1:5,000, the signal was detected by chemiluminescence (Immobilon Crescendo, Millipore) and quantified by densitometry with the Image Lab 5.2 program (Bio-Rad).

Tau solubility assay

For the extraction of insoluble Tau species with SDS, adult fly heads were homogenized in TBS/sucrose buffer (50mM Tris–HCl, pH 7.4, 175mM NaCl, 1 M sucrose, 5mM EDTA supplemented with protease and phosphatase inhibitors) as described in (Sealey *et al.* 2017, Prifti *et al.*). The samples were then spun for 2 min at 1,000 g and the supernatant was centrifuged at 200,000g for 2h at 4°C. The resulting supernatant was regarded the "soluble fraction" and the pellet was re-suspended in 5% SDS/TBS (50mM Tris–HCl pH 7.4, 175mM NaCl, 5% SDS) and centrifuged at 200,000g for 2 h at 25°C. The supernatants were collected as the SDS-soluble, aqueous-insoluble fraction. All samples were diluted in 2X Laemmli buffer and boiled for 5 min at 95°C. Equivalent volumes were loaded and analyzed by immunoblotting.

Atomic Force Microscopy (AFM)

To extract the insoluble Tau fraction enriched for filaments and excluding granular tau (GTOs), 50 adult fly heads were homogenized in TBS/sucrose (50mM Tris-HCl pH 7.4, 175mM NaCl, 1 M sucrose, 5mM EDTA and protease inhibitor cocktail) as described in (Sealey *et al.* 2017, Prifti *et al.*). The samples were then spun for 2 min at 1000g and the supernatant was centrifuged at 100,000g for 30 min at 4°C. The resulting supernatant included the aqueous soluble fraction and monomeric Tau "NS1". The pellet was re-suspended at room temperature in 5% SDS/TBS buffer and spun at 100,000g for 30 min at 25°C. The resulting "NP1" pellet was washed three times with water to remove residual SDS and re-suspended in 1X PBS. The pellet sample was placed in a freshly cleaved 10 mm mica disc (Agar Scientific) and incubated at room temperature for 5 minutes to allow absorbing. Samples were rinsed 4 times with ultrapure water and dried with compressed air. Samples were imaged in air with a digital multimode Nanoscope IV AFM operating in tapping mode with an Aluminum coated non-contact/Tapping mode probe with a resonance frequency of 320 kHz and force constant of 42N/m

(Nanoworld, POINTPROBE NHCR). Representative images were taken at random points on the sample with a scan rate of 1Hz-2Hz. The acquired images were processed by WSXM software.

Experimental Design and Statistical analyses

For all experiments, controls and experimental genotypes were tested in the same session in a balanced design. Genotypes were trained and tested in a random order. Performance indexes in behavioral experiments were analyzed parametrically with the JMP 7.1 statistical software package (SAS Institute) and plotted using Graph Pad Prism 9.5. Following an initial positive ANOVA, the means were compared to the control with planned multiple comparisons using the Least Squares Means (LSM) approach or with Dunnett's tests as indicated. Survival curves were compared at each assessment day using Wilcoxon/Kruskal-Wallis tests. The means and SEMs from each genotype for the days with significant differences were compared using the Steel with control tests. Quantification of all Western blots was performed by densitometry. Tau levels were normalized using the Syntaxin (Syx) as a loading control and are shown as a ratio of their mean ±SEM values relative to respective levels of the control genotype, which was set to 1. The means were compared following an initial positive ANOVA, using Dunnett's tests relative to the designated control. All statistical details are presented in the text and the relevant tables.

RESULTS

Deficient Protein-Synthesis-Dependent Memory upon hTau^{0N4R} accumulation in the adult CNS.

Deficient associative learning was reported to emerge in a time-dependent manner after 12 days of pan-neuronal adult-specific expression of hTau^{0N4R} (Papanikolopoulou and Skoulakis 2015, Sealey *et al.* 2017). As before (Keramidis *et al.* 2020), we used the well-established negatively reinforced olfactory conditioning assay to assess learning and consolidated memory forms (Tully *et al.* 1994). Learning was normal after 6 days of hTau^{0N4R} expression (Fig1A: ANOVA: $F_{(5,74)}$=17.6063, p=3.3x10^{-11}, subsequent LSM planned comparisons with both control strains (6days): p=0.2303 and p=0.7165 respectively), but a strong learning deficit emerged by day 12 (Fig 1A. LSM planned comparisons with both controls (12 days): p<0.0001 from both). This verified independently the previously reported (Papanikolopoulou and Skoulakis 2015) time-dependent manifestation of neuronal dysfunction in this Drosophila Tauopathy model. To determine whether deficits in consolidated memory emerge with the same time-dependence, performance was assessed 24 hrs post-training with 5 rounds of Spaced Training, known to yield Protein-Synthesis-Dependent Memory (PSD-M) (Tully *et al.* 1994). PSD-M appeared intact for 6 days of hTau expression (Fig 1B. ANOVA: $F_{(5,67)}$=10.433, p=2.7x10^{-7}, subsequent LSM planned comparisons with both controls (6days): p=0.8911 and p=0.3287 respectively). However, a robust deficit was evident after 12 days of hTau^{0N4R} expression (Fig 1B. LSM planned comparisons with both controls (12days): p=0.0025 and p=0.0089 respectively).

These robust learning and memory deficits raised the question of whether the 12-day accumulation of pathologically hyper-phosphorylated hTau^{0N4R} (Papanikolopoulou and Skoulakis 2015), affects processes underlying neuronal dysfunction specifically, or the deficits are consequent of nonspecific neurotoxicity. To probe whether flies after 12 days of hTau^{0N4R} expression are learning competent, immediate performance (learning) after 5-round Extended Conditioning of 12 CS/US pairings each (Gouzi *et al.* 2018) was assessed. This conditioning regime yielded identical learning for hTau^{0N4R}-accumulating animals and controls (Fig 1C. ANOVA: $F_{(2,40)}$=3.136, p=0.0549). Therefore, although hTau^{0N4R} accumulation in the adult Drosophila CNS compromises learning, the deficit can be rescued by over-conditioning, suggesting that it results from compromised learning rate as reported before for Drosophila mutants (Moressis *et al.* 2009), rather than ability to learn consistent with neuronal loss.

In addition, the Massed Conditioning-elicited Protein-Synthesis-Independent Memory (PSI-M) (Tully *et al.* 1994), was not affected after 12 days of hTau^{0N4R} accumulation (Fig 1D. ANOVA: $F_{(2,47)}$=3.202, p=0.0501). Because of the two consolidated memory types PSD-M is preferentially compromised, hTau^{0N4R} accumulation appears to impair translation in affected neurons, in accord to recent suggestions (Papanikolopoulou *et al.* 2019), but spares the translation-independent PSI-M. It

appears then, that adult CNS-limited hTau^{0N4R} accumulation compromises specific plasticity processes and behavioral outputs, arguing against the impairments resulting from neurotoxicity and neuronal death, which would likely affect neuroplasticity rather indiscriminately.

To verify these surprising results, two independent hTau^{0N4R}-encoding transgenes (0N4R^{a1} and 0N4R^{a2}) on different chromosomal sites (attp9A and attp86F) were generated. However, expression of both of these site-specific inserted transgenes was low and they were combined in a double transgenic strain 0N4R^{2a} to approximate hTau levels yielded by the single 0N4R transgene (Wittmann *et al.* 2001) transgene (Fig 1E. ANOVA: $F_{(3,18)}$=135.648, p=4.3x10^{-11}, subsequent LSM planned comparisons with ElavGal4;Gal80^{ts}>0N4R: p=4.9x10^{-11}, p=2.9x10^{-11} and p=2.4x10^{-5} respectively). Consistent with the results above (Fig 1A) adult specific pan-neuronal expression of hTau^{0N4R2a} for 12 days resulted in impaired learning upon a single round of 8 CS/US pairings (Fig 1F. ANOVA: $F_{(2,35)}$=143.048, p=5.5x10^{-17}, subsequent LSM planned comparisons with both controls: p=2.5x10^{-8} and p=9.5x10^{-18} respectively), which however was eliminated upon Extended Conditioning (Fig 1H. ANOVA: $F_{(2,27)}$=3.119, p=0.062). Nevertheless, this spaced conditioning regime resulted in impaired PSD-M (Fig 1G. ANOVA: $F_{(2,42)}$=13.829, p=2.7x10^{-5}, subsequent LSM planned comparisons with both controls: p=0.0001 and p= 1.9x10^{-5}), but left PSI-M intact (Fig 1I. ANOVA: $F_{(2,34)}$=2.963, p=0.0659). These results confirm with an independent transgenic strain that adult-specific pan-neuronal hTau^{0N4R} accumulation results in impaired, but not abolished associative learning and specific attenuation of PSD-M.

Tau insoluble aggregate accumulation correlates with reversal of the PSD-M deficit.

Because the effects of hTau accumulation on neuroplasticity appeared specific to PSD-M and even learning deficits were ameliorated with overtraining, we hypothesized that the CNS is unlikely to have sustained extensive neurodegenerative damage. If the fly CNS were not damaged, then repressing expression of the hTau transgene would reduce the hTau^{0N4R} load, which could attenuate the neuroplasticity deficits as in vertebrate models expressing the FTDP-linked mutant hTau^{0N4R} (Santacruz *et al.* 2005, Sydow *et al.* 2011, Van der Jeugd *et al.* 2012). To that end, adult-specific pan-neuronal hTau^{0N4R} transgene expression was permitted for 12 days at 30^{o}C as before ((Papanikolopoulou and Skoulakis 2015) and Fig 1), but it was followed by 10 days of maintaining the flies at the non-permissive for transgene expression 18^{o}C (McGuire *et al.* 2004). Another group of flies of the identical genotype were maintained as adults for 10 days at 18^{o}C and then switched to transgene-inducing 30^{o}C for 12 days (Fig 2A). Therefore, in the two groups of genotypically identical and of similar age animals, hTau^{0N4R} is either repressed for 10 days following 12 days of expression (OFF), or it is expressed for 12 days (ON) after 10 days of repression. Transgene expression levels under

these conditions were assessed on day 22 post adult emergence and revealed (Fig 2B. ANOVA: $F_{(1,13)}$=99.548, p=3.7x10^{-7}), at least a 50% reduction in *htau^{0N4R}* transcripts upon transgene repression (OFF), relative to its expression under permissive conditions (ON). In contrast protein levels remained equivalent if not somewhat elevated under transgene transcriptional repression conditions (Fig 2C. ANOVA: $F_{(1,12)}$=1.012, p=0.3327), indicating that the hTau^{0N4R} protein is rather stable in the fly CNS.

Sustained accumulation of hTau in the fly (Cowan *et al.* 2015, Papanikolopoulou and Skoulakis 2015), or vertebrate CNS (Santacruz *et al.* 2005, Wang and Mandelkow 2015) results in turnover-resistant aggregate formation. Therefore, we aimed to determine whether the apparently stable levels of hTau^{0N4R} protein under transcriptional attenuation result from aggregate accumulation. Total head lysate proteins from flies with the 0N4R and 0N4R^{2a} transgenes transcriptionally active for 12 days (ON), or inactive for 10 days (OFF), were fractionated and hTau^{0N4R} levels were quantified in the soluble and insoluble fractions. Interestingly, soluble hTau^{0N4R} levels remained unchanged, if not somewhat decreased, irrespective of whether the 0N4R and 0N4R^{2a} transgenes were ON, or OFF (Fig 2D. ANOVA: $F_{(1,11)}$=0.145, p=0.711 for hTau^{0N4R} and $F_{(1,13)}$=4.262, p=0.061 for hTau^{0N4R2a} respectively). However, insoluble hTau was elevated when the transgenes were transcriptionally inactive (Fig 2E. ANOVA: $F_{(1,11)}$=9.191, p=0.0126 for and $F_{(1,9)}$=11.556, p=0.0094 for hTau^{0N4R2a} respectively). Therefore, aggregates accumulate in the fly CNS, ostensibly formed from pre-existing soluble hTau and likely account for the apparently stable levels of the protein even after 10 days without new transgene transcription (Fig 2B).

Importantly, silencing transgene transcription (OFF) for 10 days after 12 days of expression, resulted in recovery of the PSD-M deficit compared to the significantly attenuated memory of animals expressing hTau^{0N4R} (ON). For hTau^{0N4R} (Fig 2F): ANOVA: $F_{(3,39)}$=12.466, p=9.6x10^{-6}, subsequent LSM planned comparisons with ElavG4;Gal80^{ts}>0N4R (OFF) and ElavG4;Gal80^{ts}>0N4R (ON): p=0.0015; while in comparison to w^{1118}>0N4R p=0.0099. Conversely, for hTau^{0N4R2a} (Fig 2G): ANOVA: $F_{(3,43)}$=17.761, p=1.5x10^{-7}, subsequent LSM planned comparisons with ElavG4;Gal80^{ts}>0N4R^{2a} (OFF) and ElavG4;Gal80^{ts}>0N4R^{2a} (ON): p=0.002; while in comparison to w^{1118}>0N4R^{2a} p=7.1x10^{-5}). Moreover, PSD-M was not affected by the temperature switching regimes in ElavG4;Gal80^{ts}> w^{1118} controls (Fig 2H ANOVA: $F_{(1,15)}$=0.018, p=0.8959), indicating that the differences in PSD-M in the experimental animals are not consequent of the experimental manipulations.

These results are consistent with the notion that neuronal dysfunction manifested as memory deficits, is not consequent of irreversibly damaged, or degenerating CNS neurons, but rather of reversibly impaired processes essential for PSD-M. Considering that transcriptional silencing of the transgenes elevates insoluble hTau, the results suggest that such aggregates not only do not precipitate neuronal dysfunction, but may in fact suppress, or prevent it. The deficient PSD-M could

then be mediated by newly translated, hence largely soluble hTau^{0N4R} expected in the CNS of flies expressing the transgenes for 12 days (ON).

Blocking hTau^{0N4R} insoluble aggregate formation results in defective PSD-M.

Is it hTau^{0N4R} aggregate accumulation that suppresses the PSD-M deficit, or reduction of soluble protein upon transcriptional silencing of the transgene? To differentiate between these two alternatives, we aimed to prevent hTau insoluble aggregate formation or induce their decomposition under transgene silencing conditions. To that end, flies expressing hTau^{0N4R} for 12 days at 30^{o}C were switched to the non-permissive 18^{o}C in the presence of a range of concentrations of the non-neuroleptic phenothiazine, methylene blue (MetBlu). The drug has been experimentally shown to bind to the repeat domains of hTau and inhibit hTau-hTau interactions essential for formation of insoluble aggregates (Hosokawa *et al.* 2012) and paired helical filaments (PHF) (Wischik *et al.* 1996). Since the 0N4R and 0N4R^{2a} transgenes yielded identical results in all experiments detailed above, to reduce redundancy, we used only the original randomly inserted hTau^{0N4R} transgene (Wittmann *et al.* 2001) for all subsequent experiments unless specified otherwise.

Initially we used the control genotype ElavGal4;Gal80^{ts} heterozygotes to determine the toxicity range of MetBlu at 30^{o}C, where we typically assay the longevity of hTau^{0N4R}-expressing animals (Papanikolopoulou and Skoulakis 2015, Keramidis *et al.* 2020). MetBlu in the food media at the range of 10-250μM did not affect survival significantly, but at 500 μM, it reduced the date that 50% of the population was expired (50% attrition date) (Keramidis *et al.* 2020), by 16 days and at 1mM by 22 days (Fig 3A and Table 1). Conversely, 10-100 μM of the drug did not change the 50% attrition date of hTau^{0N4R}-expressing flies relative to untreated ones but reduced it by 5 days relative to controls. The 50% attrition at 500 μM and 1mM MetBlu were shortened by 15 days and 17 days respectively, relative to untreated animals (Fig 3B and Table 2). Therefore, in agreement with prior reports (Gillman 2011), MetBlu precipitates significant concentration-dependent toxicity above 250 μM at 30^{o}C and this was more pronounced for hTau^{0N4R}-expressing flies over the range of the experiment, where the 50% attrition date for these flies at 30^{o}C was shortened by 13 days relative to their untreated siblings (Fig 3B and Table 2).

To determine the effect of the drug on the steady state levels of hTau^{0N4R} insoluble aggregates, flies expressing the transgene for 12 days were shifted to 18^{o}C to silence transcription and for these 10 days were offered food containing MetBlu ranging from 50 to 1000 μM. Head lysates from these animals were fractionated and the amount of hTau in the soluble and insoluble fractions was quantified relative to animals kept on normal food for the same period (0). Soluble hTau levels were not significantly affected by any concentration of MetBlu, but were somewhat, yet not significantly

elevated at 250 µM (Fig 3C. ANOVA: $F_{(6,40)}$=0.323, p=0.9204). Importantly, insoluble hTau^{0N4R} levels were not significantly different than controls at any MetBlu concentration except at 250 µM where they were significantly reduced (Fig 3D. ANOVA: $F_{(6,44)}$=4.142, p=0.0027. Subsequent comparisons with ElavGal4;Gal80^{ts}>0N4R OFF, revealed a significant effect of 250 µM MetBlu p=0.0008). The reason for this sharp optimum in the MetBlu concentration leading to insoluble aggregate reduction is unclear but has been consistent over a number of technical and biological experimental repeats.

Importantly, the elevated lethality of hTau^{0N4R}-expressing flies on 250 µM MetBlu (Fig 3B), was not apparent over the 10 days these animals were treated at 18^{o}C, with typical survival rates over 98% (Fig 4A. ANOVA: $F_{(19,299)}$=1.1663, p=0.042). This agrees with previous suggestions (Schirmer *et al.* 2011), that the toxicity of the drug is likely dependent on the metabolic rate. For the poikilothermic Drosophila, metabolism is expected much higher at 30 than 18^{o}C and it is most likely reflected on the lack of significant differences from controls at the lower temperature.

Significantly, immediate memory after Extended Conditioning of hTau^{0N4R}-expressing animals treated for 10 days with 250 µM MetBlu was not significantly different from untreated flies of the same genotype (Fig 4B. ANOVA: $F_{(1,15)}$=0.138, p=0.7154). However, treated animals presented a significant reduction in 24 hr PSD-M relative to untreated ones (Fig 4C. ANOVA: $F_{(1,27)}$=10.435, p=0.0033), but feeding control animals 250 µM MetBlu for 10 days did not impair PSD-M relative to that of their untreated siblings (Fig 4D. ANOVA: $F_{(1,22)}$=0.201, p=0.6584). Similarly, PSI-M was not affected in treated hTau^{0N4R}-expressing flies (Fig 4E. ANOVA: $F_{(1,29)}$=0.0016, p=0.9681). Therefore, under these conditions, the drug does not appear to precipitate non-specific dysfunction in the neurons, or mechanisms underlying PSD-M.

In support of this interpretation and disfavoring the notion of differential MetBlu-mediated dysfunction in hTau^{0N4R}-expressing flies, treatment with 500 µM of the drug, which does not appear to affect hTau aggregates (Fig 3D), did not attenuate PSD-M in hTau^{0N4R}-expressing animals (Fig 4F ANOVA $F_{(1,14)}$=2.056, p=0.1752), or in controls (Fig 4G. ANOVA: $F_{(1,23)}$=0.701, p=0.4115). Therefore, the relative elevation of aggregates upon silencing hTau^{0N4R} transcription likely accounts for the resultant reversal of PSD-M deficits (Fig 2F, G). The collective results strongly argue that while hTau^{0N4R} aggregates are benign, or protective, the smaller apparently soluble protein species are deleterious to processes requisite for PSD-M.

Efficient PSD-M in hTau^{0N3R}-expressing flies correlates with elevated aggregates and is reversible with MetBlu.

Unlike for hTau^{0N4R} expressing flies, associative learning and PSD-M are normal in animals expressing the hTau^{0N3R} isoform even after 12 days of transgene induction (Sealey *et al.* 2017).

Quantification of insoluble hTau^{0N3R} in head lysates revealed a nearly 6-fold elevation over aggregates in lysates from hTau^{0N4R} animals after 12 days at 30^{o}C (Fig 5A. ANOVA: $F_{(1,9)}$=51.036, p=9.8x10^{-5}). Considering the results above, this difference led to the hypothesis that the reported lack of learning and memory defects in hTau^{0N3R}-expressing animals is a consequence of the elevated steady state aggregates. To address this hypothesis, hTau^{0N3R}-expressing animals were subjected to MetBlu-mediated aggregation inhibition for the 12 days the transgene was actively transcribed post eclosion.

As reported before (Sealey *et al.* 2017), hTau^{0N3R}-expressing animals presented significantly reduced survival at 30^{o}C and this premature mortality was exaggerated by MetBlu at concentrations higher than 10 µM (Table 3), likely due to enhanced metabolism at the higher temperature (Schirmer *et al.* 2011). Treatment with the less toxic MetBlu concentrations over the 12 days of hTau^{0N3R} expression in adults, did not affect significantly the levels of soluble hTau^{0N3R} (Fig 5B. ANOVA: $F_{(3,15)}$=0.495, p=0.6927). However, the levels of insoluble hTau^{0N3R} were significantly different on 50 µM MetBlu and appeared reduced on the other concentrations assayed as well (Fig 5B. ANOVA: $F_{(3,48)}$=3.013, p=0.0397, subsequent comparisons with untreated p=0.0044). As expected, survival of hTau^{0N3R}-expressing flies on 50 µM MetBlu was reduced by the 12th day at 30^{o}C, but not earlier (Fig 5C. ANOVA: $F_{(23,407)}$=8.534, p=5.1x10^{-23}, subsequent planned comparisons: 12-day treated ElavGal4;Gal80^{ts} heterozygotes *versus* treated ElavGal4;Gal80^{ts}>0N3R: p=2.4x10^{-6}, but p=0.0002 for the same comparison at 8 days and p=0.0271 at 6 days). Further survival reduction by MetBlu suggests that toxicity is not affected by insoluble hTau^{0N3R} accumulation, but rather results from the newly translated upon transgene induction soluble protein, or the accumulation of oligomeric species due to MetBlu mediated aggregation inhibition.

If the elevated insoluble species are indeed responsible for the lack of PSD-M deficits after 12 days of 0N3R transgene induction as hypothesized, then memory deficits are expected to emerge upon MetBlu-mediated aggregate attenuation. Therefore, hTau^{0N3R}-expressing flies were kept on 50 µM MetBlu-containing media, which was effective at attenuating aggregates (Fig 5B), for the 12 days of adult transgene expression. This treatment did not affect Immediate Memory after Extended Conditioning (Fig 5D. ANOVA: $F_{(1,23)}$=0.107, p=0.7470) compared to untreated congenic animals. However, PSD-M (Fig 5E) was significantly reduced (ANOVA: $F_{(1,28)}$=9.407, p=0.0049) by 50 µM MetBlu treatment, while PSI-M remained unaffected (Fig 5F. ANOVA: $F_{(1,20)}$=4.120, p=0.0566). The specificity of the impairment only for PSD-M suggests that the deficit is unlikely the result of nonspecific drug toxicity. To ascertain this, control animals were kept on 50 µM MetBlu for 12 days at 30^{o}C, which does not impact their survival (Fig 3A), nor their PSD-M performance relative to that of untreated flies (Fig 5G. ANOVA: $F_{(1,28)}$=0.113, p=0.7397). This provides independent validation that the deficit in hTau^{0N3R}-expressing flies upon 50 µM MetBlu treatment is not consequent of drug toxicity. Furthermore, PSD-

M was not affected in hTau^{0N3R}-expressing flies kept on 10 µM (Fig 5H. ANOVA: $F_{(1,25)}$=0.007, p=0.936), or 100 µM MetBlu (Fig 5I. ANOVA: $F_{(1,23)}$=0.571, p=0.458), conditions that do not significantly reduce aggregates (Fig 5B).

Therefore, memory deficits emerge in hTau^{0N3R}-expressing animals only under conditions that attenuate aggregate formation, independently confirming that aggregation of this hTau isoform is also not inhibitory and may in fact be permissive to PSD-M. Accordingly, the deficient PSD-M presented by hTau^{0N4R}-expressing animals kept at 30^{o}C for 12 days was further significantly decreased if these animals were simultaneously kept at 50 µM (Fig 5J. ANOVA: $F_{(1,23)}$=7.211, p=0.0135), but was not affected if flies were kept on 100 µM MetBlu (Fig 5K. ANOVA: $F_{(1,22)}$=2.576, p=0.1234), both concentrations that do not affect their survival (Fig 3B), but only the former inhibiting aggregation. Therefore, inhibiting insoluble aggregate formation of two different hTau isoforms in the Drosophila CNS results in specific PSD-M deficits.

The size and abundance of aggregates in their CNS correlate with the memory deficits in hTau^{0N4R} and hTau^{0N3R}-expressing animals.

To independently verify the results supporting the notion that hTau aggregation does not impair, but rather may be permissive to processes required for PSD-M formation, storage or recall, insoluble Tau species were recovered from adult head lysates as detailed before (Cowan *et al.* 2015, Sealey *et al.* 2017), placed on mica disks and their sizes and configurations examined under Atomic Force Microscopy (AFM) are summarized in Figure 6.

In agreement with transgene expression (Fig 2B) and biochemical assessment (Fig 3C, D), induction of the hTau^{0N4R} isoforms yielded few and rather small (<40nm) apparent aggregates (Fig 6A.1). Significantly, maintaining the flies under conditions restrictive to transgene expression, following initial induction resulted in accumulation of very large aggregates (>300nm width) in the CNS of these animals (Fig 6A.2-large arrowhead). However, these aggregates appeared highly reduced both in size and abundance if hTau^{0N4R}-expressing flies were maintained on 250µM MetBlu-laced food during this period (Fig 6A.3) and some appeared filamentous in shape (Fig 6A.3-star). Therefore, these results agree with the biochemically detectable aggregate accumulation upon transgene silencing (Fig 2E), the effect of maintaining the animals on 250µM MetBlu on aggregates (Fig 3D) and the emergence of PSD-M deficits in the latter animals (Fig 4C).

Conversely, medium aggregates (50-80nM) were apparent in CNS lysates of hTau^{0N3R}-expressing flies (Fig 6B.1). These were highly reduced in abundance and size if these transgene-expressing animals were simultaneously maintained on 50µM MetBlu-laced food (Fig 6B.2). Interestingly, maintaining these animals on 100 µM MetBlu, which did not affect their PSD-M

performance (Fig 5I), or the level of biochemically-detected aggregates (Fig 5B), did not appear to affect the abundance or size of the aggregates and appeared conducive to formation of filamentous forms of the protein (Fig 6B.3-star).

Collectively, these results provide additional support to the conclusion that large hTau aggregates do not impair processes requisite for PSD-M, but the smaller, likely soluble aggregates do. Therefore, the presence of aggregates correlates with comparatively normal PSD-M formation.

Aggregates in adult mushroom body neurons do not impair PSD-M.

The mushroom body neurons (MBs) are implicated in PSD-M formation and recall (Davis 2005, Cognigni *et al.* 2018) and relatively low chronic Tau expression therein has been reported to precipitate learning and short-term memory deficits, while leaving these neurons structurally intact in the short term (Mershin *et al.* 2004). However, whether adult-specific hTau expression within these neurons results in consolidated memory deficits, in a manner analogous to those observed in human sporadic Tauopathy patients, has not been examined systematically.

To determine whether PSD-M is compromised by adult-specific hTau^{0N4R} accumulation within these neurons, this hTau isoform was specifically expressed in adults under the strong pan-MB neuron driver LeoGal4 (Messaritou *et al.* 2009) for 12 days post-eclosion. Surprisingly, expression levels of hTau^{0N4R} under LeoGal4 were highly elevated compared to those expressing pan-neuronally under ElavGal4 (Fig 7A. ANOVA: $F_{(1,11)}$=37.416, p=0.0001) and this was verified independently with the hTau^{0N4R2a} double transgenic strain (Fig 7B. ANOVA: $F_{(1,11)}$=34.926, p=0.0001). This is surprising considering the small number of neurons expressing hTau under LeoGal4 (Messaritou *et al.* 2009) compared to pan-neuronal expression under ElavGal4 (Robinow and White 1988) and indicates that a large excess of hTau accumulates within these ~4000 MB neurons (Aso *et al.* 2009) during the 12 days of transgene expression. However, despite this vast hTau accumulation, PSD-M was unaffected both in hTau^{0N4R} (Fig 7C. ANOVA: $F_{(2,39)}$=1.527, p=0.2306) and hTau^{0N4R2a}-expressing (Fig 7D. ANOVA: $F_{(2,39)}$=2.706, p=0.0799) animals. These data support the notion that expression levels alone do not correlate with and predict neuronal dysfunction.

As for the soluble 0N4R, insoluble species were highly abundant in head lysates of hTau^{0N4R}-expressing flies under LeoGal4, compared to those under ElavGal4 (Fig 7E. ANOVA for Soluble: $F_{(1,11)}$=291.294.499, p=1.0x10^{-8} and ANOVA for Insoluble: $F_{(1,11)}$=49.499, p=3.6x10^{-5}), suggesting that in accord with the results and the hypothesis above, their accumulation could suppress hTau-dependent dysfunction of MB neurons. Given the dependence of MetBlu toxicity on temperature and hence fly metabolism and the rather limited number of neurons targeted, we opted to inhibit aggregate formation with 10 µM MetBlu, a concentration without significant effects on the viability of control

(Fig 3A) or flies expressing $hTau^{0N4R}$ pan-neuronally (Fig 3B). Hence, MetBlu at 10μM was fed to adult flies during the 12days of transgene expression to inhibit aggregate formation and address the hypothesis-borne prediction that this treatment will result in PSD-M deficits. Indeed, MetBlu treatment did not affect learning/immediate memory after Extended Conditioning (Fig 7F. ANOVA: $F_{(1,23)}$=0.719, p=0.4797), indicating the expected lack of toxicity of 10μM MetBlu. In contrast, PSD-M was significantly impaired in animals expressing $hTau^{0N4R}$ (Fig 7G. ANOVA: $F_{(1,23)}$=6.768, p=0.0163), or $hTau^{0N4R2a}$ (Fig 7H. ANOVA: $F_{(1,23)}$=6.192, p=0.0209) in their MBs compared to untreated controls, which presented memory levels in the expected normal range. Therefore, insoluble hTau aggregate accumulation within the MBs, even at the excessive levels under LeoGal4, do not precipitate neuronal dysfunction manifested as PSD-M deficits in contrast to soluble species that ostensibly do.

DISCUSSION

Reversal of adult onset hTau-driven neuroplasticity deficits.

Time-dependent memory deficits likely reflective of disease progression, characterize most sporadic Tauopathies involving non-mutated Tau, such as AD (Lee *et al.* 2001, Delacourte 2005). This time dependence of associative learning and PSD-M attenuation is clearly emulated in our adult onset hTau transgene expression model (Fig 1 and (Sealey *et al.* 2017)). However, it has been unclear whether these cognitive deficits are the consequence of irreversibly dysfunctional or degenerating neurons. Evidence from regulatable expression transgenic mouse models expressing the FTDP-linked mutations P301L and ΔK280 in the 0N4R isoform indicated that switching off hTau expression improved the associated memory impairment, without a reduction in large aggregates (Santacruz *et al.* 2005, Sydow *et al.* 2011, Van der Jeugd *et al.* 2012).

To our knowledge, this report is the first to demonstrate reversal of memory deficits upon attenuation of wild type hTau expression. Together with the mouse data, these results support the hypothesis that learning and PSD-M deficits are not consequent of irreversibly damaged neurons expressing wild type of mutant hTau isoforms. Rather, cognitive deficits result from dysfunctional, but otherwise apparently healthy neurons and therefore may be pharmacologically reversible in patients as well, at least prior to later degenerative stages of the disease (Braak and Braak 1996, Lee *et al.* 2001, Papanikolopoulou and Skoulakis 2020).

Significantly, we also demonstrate that excess 0N3R or 0N4R hTau in the fly CNS specifically compromise the apparent rate of learning and PSD-M but learning *per se* and PSI-M remain intact. These results add further credence to the interpretation that excess hTau alone does not result in generally dysfunctional fly CNS, but rather it compromises specific processes and mechanisms essential for protein synthesis-dependent consolidated memory. Because recall of PSD-M requires neurotransmission from the MBs in Drosophila (McGuire *et al.* 2001), it appears likely that the compromised memory when soluble hTau expression is limited to the MBs (Fig 7G,H) reflects deficits in synaptic function as previously proposed (Wang and Mandelkow 2015).

Why does accumulation of ostensibly small soluble hTau aggregates impair PSD-M? Direct evidence of a physiological function of Tau as a negative regulator of translation was uncovered for the homologous Drosophila protein. Knock-out mutants of dTau present elevated translation and enhanced PSD-M, while overexpression of the protein impairs both processes (Papanikolopoulou *et al.* 2019). Therefore, elevation of small insoluble hTau aggregates likely impairs translation and precipitates the specific PSD-M deficits, but spares the translation independent memory (PSI-M). PSI-M has also been reported to depend at least in part on regulated filamentous actin (F-actin) stability

(Kotoula *et al.* 2017). Excess hTau in the fly CNS has been reported to stabilize F-actin (Fulga *et al.* 2007), providing a plausible explanation as to why PSI-M remains intact under these conditions.

Adult CNS-specific hTau aggregation correlates with suppression of neuroplasticity deficits.

In agreement with the FTDP mouse models (Santacruz *et al.* 2005, Sydow *et al.* 2011, Van der Jeugd *et al.* 2012), aggregates not only persist in Drosophila for at least 10 days after transgene silencing, but apparently comprise a significant fraction of the $hTau^{0N4R}$ isoform in the fly CNS (Fig 2E). Conversely, insoluble species make up a significant fraction of the $hTau^{0N3R}$ isoform in the fly CNS even when this transgene is fully transcriptionally active for 12 days (Fig 5A). The greater aggregation propensity of $hTau^{0N3R}$ may reflect its elevated phosphorylation state relative to its $hTau^{0N4R}$ counterpart in the Drosophila CNS (Sealey *et al.* 2017), and/or its reduced affinity for microtubules. Either of these scenarios likely renders a significant number of $hTau^{0N3R}$ proteins more prone to aggregation (Goode *et al.* 2000). A large increase in insoluble $hTau^{0N4R}$ without silencing the transgene was observed when expression of this isoform was confined to the ~4500 MB neurons with the very strong LeoGal4 driver, relative to the levels attained under similar conditions with the pan-neuronally expressed (~$1x10^5$ neurons) ElavGal4 (Fig 7E). This clearly demonstrates that aggregation is favored by excessive local hTau accumulation as within the confines of particular neurons in agreement with *in vitro* experiments (Montejo de Garcini *et al.* 1986, von Bergen *et al.* 2005).

Insoluble hTau aggregates have been linked to neurodegenerative Tauopathies (Delacourte and Buee 2000, Geschwind 2003, Trojanowski and Lee 2005) and larger ones such as NFTs may in fact contribute to toxicity in later stages of the disease. However evidence supporting a cardinal role for soluble Tau oligomers in neuronal dysfunction and toxicity has been increasing (Cowan and Mudher 2013, Cowan *et al.* 2015), while direct evidence for the role of large insoluble aggregates in these processes remains scant (Cowan *et al.* 2015, Wang and Mandelkow 2015, Arendt *et al.* 2016). In addition, aggregates are relatively abundant in patients with Primary Age Related Tauopathy (PART), but these individuals seldom present cognitive deficits (Jellinger 2015, Jellinger *et al.* 2015). Neurons may in fact degenerate when they are devoid of NFTs (Wittmann *et al.* 2001, Papanikolopoulou and Skoulakis 2011, Wang and Mandelkow 2015) and this is a hypothesis currently under investigation in our fly model.

The data herein provide three experimental scenarios strongly supporting the view that insoluble aggregates, whose exact conformation(s) are unclear at the moment, are protective or permissive of neuronal activities that underlie associative PSD-M. Our data extend the findings from regulatable mouse FTDP models that aggregates remain, while cognition improves (Santacruz *et al.* 2005, Sydow *et al.* 2011, Van der Jeugd *et al.* 2012), to posit that insoluble aggregates are in fact

permissive if not protective of neuroplasticity. The results from the three experimental scenarios supporting this notion are discussed below.

Silencing the transgene in hTau^{0N4R}-expressing animals results in reversal of their PSD-M deficit and in fact correlates well with an increase in large insoluble aggregates (Fig 2F, G, Fig 6A.2). In contrast, the PSD-M deficit was sustained by MetBlu-mediated inhibition of aggregation after transgene silencing (Fig 4C, Fig 6A.3). In accord with this, MetBlu concentrations that do not affect hTau^{0N4R} aggregation were not deleterious to PSD-M (Fig 4F). Moreover, inhibition of aggregation while the hTau^{0N4R} transgene was expressed, exaggerated the PSD-M deficit of these flies (Fig 5J). In the MB-limited expression setting, hTau^{0N4R} the excessive aggregates within these neurons (Fig 7E) are the likely reason that PSD-M remained normal after 12 days of transgene expression (Fig 7C, D), but was compromised after MetBlu mediated inhibition of aggregation (Fig 7G, H). Finally, in the case of hTau^{0N3R}adult-specific expression reported to spare learning and PSD-M (Sealey *et al.* 2017), we now provide evidence that this correlates nicely with the relative abundance of aggregates (Fig 5A,B, Fig 6B1), as MetBlu-mediated inhibition of their formation precipitated robust PSD-M deficits (Fig 5E, Fig 6B.2).

Collectively therefore, insoluble hTau aggregates in the fly CNS at least, do not impair neuronal processes requisite for efficient learning and PSD-M such as regulated translation. This agrees with the suggestion that aggregate formation may reflect protective cellular response(s) to excess hyperphosphorylated Tau (Wang and Mandelkow 2015). Conversely, our data support the idea that small soluble oligomers, or monomeric to trimeric hTau species impede essential for PSD-M neuroplasticity. Oligomeric hTau may also be the neurotoxicity culprit, as inhibiting hTau aggregation at relatively low MetBlu concentrations (50-250 μM), with minimal effect on control flies (Fig 3A), under increased metabolic conditions (30^{o}C), yielded highly significant reduction in the life span of flies expressing hTau isoforms (Fig 3B, Table 2). Therefore, inhibition of aggregation with the resultant excess of oligomeric species or both, are also toxic to the CNS, precipitating premature lethality.

Preventive (Hochgräfe *et al.* 2015), or therapeutic (Santacruz *et al.* 2005, Sydow *et al.* 2011, Van der Jeugd *et al.* 2012) treatment with MetBlu in mouse models of FTDP recovers cognition. However, the effects of the drug on a *bona fide* mouse AD models have not been assessed to our knowledge. In contrast, MetBlu has been tried on patients, even in Phase III trials as an anti-aggregation therapeutic for AD with very poor results (Gauthier *et al.* 2016), most likely because it does not inhibit soluble Tau species including small oligomers (Soeda *et al.* 2015), which apparently accumulate to high levels. Furthermore, recent results from a mouse FTDP model, indicate that soluble hTau oligomers carrying the P301L mutation appear solely responsible for Tauopathy progression (Shin *et al.* 2020). Collectively then and in light of our own results, aggregation promoting

pharmaceuticals (Dominguez-Meijide *et al.* 2020) should be considered with caution as they can easily lead to dispersal of larger protective tau species to increase the availability of the toxic smaller soluble oligomers. Conversely pharmaceutical agents that may encourage the sequestration of toxic smaller oligomers into innocuous larger aggregates should be explored.

ACKNOWLEDGEMENTS

We thank the Bloomington Drosophila Stock Center for stocks, Dr. Martin Chow (University of Kentucky) for the 0N4R cDNA, Dr K. Papanikolopoulou (BSRC Alexander Fleming) for significant help with construction of the double transgenic line, M. Loizou (BSRC Alexander Fleming) for technical help and Dr Iris Nandhakumar (University of Southampton) for help with the Atomic Force Microscopy experiments. This research was supported in part by the "InfrafrontierGR/Phenotypos: The Greek Research Infrastructure for Molecular and Behavioral Phenotyping of biological model organisms for chronic degenerative diseases (MIS: 5002135), co-financed by Greece and the European Union - European Regional Development Fund and the Flagship Initiative for Neurodegenerative Diseases Research on the Basis of Precision Medicine, in the framework of the project "Infrastructures for National Research Networks for Precision Medicine and Climate Change" no. 2018ΣΕ01300001 of the General Secretariat for Research and Innovation National Public Investments Programme.

CONFLICT OF INTEREST

The authors declare no conflict of interest.

REFERENCES

Alonso, A., T. Zaidi, M. Novak, I. Grundke-Iqbal and K. Iqbal (2001). "Hyperphosphorylation induces self-assembly of tau into tangles of paired helical filaments/straight filaments." Proc Natl Acad Sci U S A **98**(12): 6923-6928.

Andorfer, C., C. M. Acker, Y. Kress, P. R. Hof, K. Duff and P. Davies (2005). "Cell-cycle reentry and cell death in transgenic mice expressing nonmutant human tau isoforms." J Neurosci **25**(5446-5454.).

Andreadis, A., J. A. Broderick and K. S. Kosik (1995). "Relative exon affinities and suboptimal splice site signals lead to non-equivalence of two cassette exons." Nucleic Acids Res **23**(17): 3585-3593.

Arendt, T., J. T. Stieler and M. Holzer (2016). "Tau and tauopathies." Brain Res Bull **126**(Pt 3): 238-292.

Aso, Y., K. Grubel, S. Busch, A. B. Friedrich, I. Siwanowicz and H. Tanimoto (2009). "The mushroom body of adult Drosophila characterized by GAL4 drivers." J Neurogenet **23**(1-2): 156-172.

Bischof, J., R. K. Maeda, M. Hediger, F. Karch and K. Basler (2007). "An optimized transgenesis system for Drosophila using germ-line-specific phiC31 integrases." Proc Natl Acad Sci U S A **104**(9): 3312-3317.

Braak, H. and E. Braak (1996). "Development of Alzheimer-related neurofibrillary changes in the neocortex inversely recapitulates cortical myelogenesis." Acta Neuropathol (Berl) **92**(2): 197-201.

Cognigni, P., J. Felsenberg and S. Waddell (2018). "Do the right thing: neural network mechanisms of memory formation, expression and update in Drosophila." Curr Opin Neurobiol. **49**: 51-58.

Cowan, C. M. and A. Mudher (2013). "Are tau aggregates toxic or protective in tauopathies?" Front Neurol. **4**(doi: 10.3389/fneur.2013.00114. eCollection 2013).

Cowan, C. M., S. Quraishe, S. Hands, M. Sealey, S. Mahajan, D. W. Allan and A. Mudher (2015). "Rescue from tau-induced neuronal dysfunction produces insoluble tau oligomers." Sci Rep **5**: 17191.

Davis, R. L. (2005). "Olfactory memory formation in Drosophila: From Molecular to systems Neuroscience." Annu. Rev. Neurosci. **28**: 275-302.

Delacourte, A. (2005). "Tauopathies: recent insights into old diseases." Folia Neuropathologica **43**(4): 244-257.

Delacourte, A. and L. Buee (2000). "Tau pathology: a marker of neurodegenerative disorders." Curr Opin Neurol **13**(4): 371-376.

Dominguez-Meijide, A., E. Vasili and T. Outeiro (2020). "Pharmacological Modulators of Tau Aggregation and Spreading." Brain Sci. **10**(11): 858.

Fulga, T. A., I. Elson-Schwab, V. Khurana, M. L. Steinhilb, T. L. Spires, B. T. Hyman and M. B. Feany (2007). "Abnormal bundling and accumulation of F-actin mediates tau-induced neuronal degeneration in vivo." Nat Cell Biol. **9**(2): 139-148.

Gauthier, S., H. Feldman, L. Schneider, G. Wilcock, G. Frisoni, J. Hardlund, H. Moebius, P. Bentham, K. Kook, D. Wischik, B. Schelter, C. Davis, R. Staff, L. Bracoud, K. Shamsi, J. Storey, C. Harrington and C. Wischik (2016). "Efficacy and safety of tau-aggregation inhibitor therapy in patients with mild or moderate Alzheimer's disease: a randomised, controlled, double-blind, parallel-arm, phase 3 trial." Lancet. **388**(10062): 2873-2884.

Geschwind, D. H. (2003). "Tau phosphorylation, tangles, and neurodegeneration: the chicken or the egg?" Neuron **40**(3): 457-460.

Gillman, P. (2011). "CNS toxicity involving methylene blue: the exemplar for understanding and predicting drug interactions that precipitate serotonin toxicity." J Psychopharmacol. **25**: 429-436.

Giong, H., M. Subramanian, K. Yu and J. Lee (2021). "Non-Rodent Genetic Animal Models for Studying Tauopathy: Review of Drosophila, Zebrafish, and C. elegans Models." Int J Mol Sci. **22**(16): 8465.

Goode, B., M. Chau, P. Denis and S. Feinstein (2000). "Structural and functional differences between 3-repeat and 4-repeat tau isoforms. Implications for normal tau function and the onset of neurodegenetative disease." J Biol Chem. **275**(49): 38182-38189.

Gouzi, J. Y., M. Bouraimi, I. G. Roussou, A. Moressis and E. M. C. Skoulakis (2018). "The Drosophila Receptor Tyrosine Kinase Alk Constrains Long-Term Memory Formation." J Neurosci **38**(35): 7701-7712.

Hochgräfe, K., A. Sydow, D. Matenia, D. Cadinu, S. Könen, O. Petrova, M. Pickhardt, P. Goll, F. Morellini, E. Mandelkow and E. Mandelkow (2015). "Preventive methylene blue treatment preserves cognition in mice expressing full-length pro-aggregant human Tau." Acta Neuropathol Commun **3**: 25.
Hosokawa, M., T. Arai, M. Masuda-Suzukake, T. Nonaka, M. Yamashita, H. Akiyama and M. Hasegawa (2012). "Methylene blue reduced abnormal tau accumulation in P301L tau transgenic mice." PLoS One. **7**(12): e52389.
Jellinger, K. (2015). "Primary age-related tauopathy (PART) and Alzheimer's disease (AD)." Alzheimers Dement. **15**(5): 720.
Jellinger, K., I. Alafuzoff, J. Attems, T. Beach, N. Cairns, J. Crary, D. Dickson, P. Hof, B. Hyman, C. J. Jack, G. Jicha, D. Knopman, G. Kovacs, I. Mackenzie, E. Masliah, T. Montine, P. Nelson, F. Schmitt, J. Schneider, A. Serrano-Pozo, D. Thal, J. Toledo, J. Trojanowski, J. Troncoso, J. Vonsattel and T. Wisniewski (2015). "PART, a distinct tauopathy, different from classical sporadic Alzheimer disease. ." Acta Neuropathol. **129**(5): 757-762.
Kaniyappan, S., R. Chandupatla, E. Mandelkow and E. Mandelkow (2017). "Extracellular low-n oligomers of tau cause selective synaptotoxicity without affecting cell viability." **13**(11): 1270-1291.
Keramidis, I., E. Vourkou, K. Papanikolopoulou and E. Skoulakis (2020). "Functional interactions of Tau phosphorylation sites that mediate toxicity and deficient learning in Drosophila melanogaster " Front. Molecc. Neurosci **In Press**.
Kosmidis, S., S. Grammenoudi, K. Papanikolopoulou and E. M. C. Skoulakis (2010). "Differential effects of Tau on the integrity and function of neurons essential for learning in Drosophila." J. Neurosci. **30**: 464-477.
Kotoula, V., A. Moressis, O. Semelidou and E. M. C. Skoulakis (2017). "Drk-mediated signaling to Rho kinase is required for anesthesia-resistant memory in Drosophila." Proc Natl Acad Sci U S A **114**(41): 10984-10989.
Lee, V. M.-Y., M. Goedert and J. Q. Trojanowski (2001). "Neurodegenerative tauopathies." Annu. Rev. Neurosci. **24**: 1121–1159.
McGuire, S., P. Le and D. RL. (2001). "The role of Drosophila mushroom body signaling in olfactory memory. ." Science. **293**(5533): 1330-1333.
McGuire, S. E., Z. Mao and R. L. Davis (2004). "Spatiotemporal gene expression targeting with the TARGET and gene-switch systems in Drosophila." Sci STKE **2004**(220): pl6.
McGuire, S. E., G. Roman and R. L. Davis (2004). "Gene expression systems in Drosophila: a synthesis of time and space." Trends Genet **20**(8): 384-391.
Mershin, A., E. Pavlopoulos, O. Fitch, B. C. Braden, D. V. Nanopoulos and E. M. Skoulakis (2004). "Learning and memory deficits upon TAU accumulation in Drosophila mushroom body neurons." Learn Mem **11**(3): 277-287.
Messaritou, G., F. Leptourgidou, M. Franco and E. M. Skoulakis (2009). "A third functional isoform enriched in mushroom body neurons is encoded by the Drosophila 14-3-3zeta gene." FEBS Lett **583**(17): 2934-2938.
Moressis, A., Friedrich, A. R., Pavlopoulos E., Davis, R. L. and E. M.C. Skoulakis. (2009) A dual role for the adaptor protein DRK in Drosophila olfactory learning and memory. J. Neurosci. **29**:2611-2625
Montejo de Garcini, E., L. Serrano and J. Avila (1986). "Self assembly of microtubule associated protein tau into filaments resembling those found in Alzheimer disease." Biochem Biophys Res Commun. **141**(2): 790-796.
Papanikolopoulou, K., I. G. Roussou, J. Y. Gouzi, M. Samiotaki, G. Panayotou, L. Turin and E. M. C. Skoulakis (2019). "Drosophila Tau Negatively Regulates Translation and Olfactory Long-Term Memory, But Facilitates Footshock Habituation and Cytoskeletal Homeostasis." J Neurosci **39**(42): 8315-8329.
Papanikolopoulou, K. and E. M. Skoulakis (2011). "The power and richness of modelling tauopathies in Drosophila." Mol Neurobiol **44**(1): 122-133.
Papanikolopoulou, K. and E. M. Skoulakis (2015). "Temporally distinct phosphorylations differentiate Tau-dependent learning deficits and premature mortality in Drosophila." Hum Mol Genet **24**(7): 2065-2077.

Papanikolopoulou, K. and E. M. C. Skoulakis (2020). "Altered Proteostasis in Neurodegenerative Tauopathies." Adv Exp Med Biol **1233**: 177-194.
Patterson, K., C. Remmers, Y. Fu, S. Brooker, N. Kanaan, L. Vana, S. Ward, J. Reyes, K. Philibert, M. Glucksman and L. Binder (2011). "Characterization of prefibrillar Tau oligomers in vitro and in Alzheimer disease." J Biol Chem. **286**(26): 23063-23076.
Prifti, E., E. Tsakiri, E. Vourkou, G. Stamatakis, M. Samiotaki and K. Papanikolopoulou (2022). "The Two Cysteines of Tau Protein Are Functionally Distinct and Contribute Differentially to Its Pathogenicity in Vivo." J Neurosci. **41**(4): 797-810.
Robinow, S. and K. White (1988). "The locus elav of Drosophila melanogaster is expressed in neurons at all developmental stages." Dev Biol **126**(2): 294-303.
Sahara, N., S. Maeda, M. Murayama, T. Suzuki, N. Dohmae, S. H. Yen and A. Takashima (2007). "Assembly of two distinct dimers and higher-order oligomers from full-length tau." Eur J Neurosci **25**(10): 3020-3029.
Sahara, N., S. Maeda and A. Takashima (2008). "Tau oligomerization: a role for tau aggregation intermediates linked to neurodegeneration." Curr Alzheimer Res **5**(6): 591-598.
Santacruz, K., J. Lewis, T. Spires, J. Paulson, L. Kotilinek, M. Ingelsson, A. Guimaraes, M. DeTure, M. Ramsden, E. McGowan, C. Forster, M. Yue, J. Orne, C. Janus, A. Mariash, M. Kuskowski, B. Hyman, M. Hutton and K. H. Ashe (2005). "Tau suppression in a neurodegenerative mouse model improves memory function." Science **309**(5733): 476-481.
Schirmer, R., H. Adler, M. Pickhardt and E. Mandelkow (2011). ""Lest we forget you--methylene blue..."." Neurobiol Aging. **32**(12): 2325.e2327-2316.
Sealey, M. A., E. Vourkou, C. M. Cowan, T. Bossing, S. Quraishe, S. Grammenoudi, E. M. C. Skoulakis and A. Mudher (2017). "Distinct phenotypes of three-repeat and four-repeat human tau in a transgenic model of tauopathy." Neurobiol Dis **105**: 74-83.
Shi, Y., W. Zhang, Y. Yang, A. Murzin, B. Falcon, A. Kotecha, M. van Beers, A. Tarutani, F. Kametani, H. Garringer, R. Vidal, G. Hallinan, T. Lashley, Y. Saito, S. Murayama, M. Yoshida, H. Tanaka, A. Kakita, T. Ikeuchi, A. Robinson, D. Mann, G. Kovacs, T. Revesz, B. Ghetti, M. Hasegawa, M. Goedert and S. Scheres (2021). "Structure-based classification of tauopathies." Nature **598**(7880): 359-363.
Shiells, H., B. Schelter, P. Bentham, T. Baddeley, C. Rubino, H. Ganesan, J. Hammel, V. Vuksanovic, R. Staff, A. Murray, L. Bracoud, D. Wischik, G. Riedel, S. Gauthier, J. Jia, H. Moebius, J. Hardlund, C. Kipps, K. Kook, J. Storey, C. Harrington and C. Wischik (2020). "Concentration-Dependent Activity of Hydromethylthionine on Clinical Decline and Brain Atrophy in a Randomized Controlled Trial in Behavioral Variant Frontotemporal Dementia." J Alzheimers Dis. **75**(2): 501-519.
Shin, S., D. Kim, J. Song, H. Jeong, S. Hyeon, N. Kowall, H. Ryu, A. Pae, S. Lim and Y. Kim (2020). "Visualization of soluble tau oligomers in TauP301L-BiFC transgenic mice demonstrates the progression of tauopathy." Prog Neurobiol. **Feb 24**: 101782.
Soeda, Y., M. Yoshikawa, O. F. Almeida, A. Sumioka, S. Maeda, H. Osada, Y. Kondoh, A. Saito, T. Miyasaka, T. Kimura, M. Suzuki, H. Koyama, Y. Yoshiike, H. Sugimoto, Y. Ihara and A. Takashima (2015). "Toxic tau oligomer formation blocked by capping of cysteine residues with 1,2-dihydroxybenzene groups." Nat Commun **6**: 10216.
Sotiropoulos, I., M. C. Galas, J. M. Silva, E. Skoulakis, S. Wegmann, M. B. Maina, D. Blum, C. L. Sayas, E. M. Mandelkow, E. Mandelkow, M. G. Spillantini, N. Sousa, J. Avila, M. Medina, A. Mudher and L. Buee (2017). "Atypical, non-standard functions of the microtubule associated Tau protein." Acta Neuropathol Commun **5**(1): 91.
Spillantini, M. G. and M. Goedert (1998). "Tau protein pathology in neurodegenerative diseases." Trends Neurosci **21**(10): 428-433.
Spires-Jones, T., K. Kopeikina, R. Koffie, A. de Calignon and B. Hyman (2011). "Are tangles as toxic as they look?" J Mol Neurosci. **45**(3): 438-444.
Spires-Jones, T., W. Stoothoff, A. de Calignon, P. Jones and B. Hyman (2009). "Tau pathophysiology in neurodegeneration: a tangled issue." Trends Neurosci. **32**(3): 150-159.

Sydow, A., A. Van der Jeugd, F. Zheng, T. Ahmed, D. Balschun, O. Petrova, D. Drexler, L. Zhou, G. Rune, E. Mandelkow, R. D'Hooge, C. Alzheimer and E. M. Mandelkow (2011). "Tau-induced defects in synaptic plasticity, learning, and memory are reversible in transgenic mice after switching off the toxic Tau mutant." J Neurosci **31**(7): 2511-2525.
Trojanowski, J. Q. and V. M. Lee (2005). "Pathological tau: a loss of normal function or a gain in toxicity?" Nat Neurosci **8**(9): 1136-1137.
Tully, T., T. Preat, S. C. Boynton and M. Del Vecchio (1994). "Genetic dissection of consolidated memory in Drosophila." Cell **79**(1): 35-47.
Van der Jeugd, A., K. Hochgräfe, T. Ahmed, J. M. Decker, A. Sydow, A. Hofmann, D. Wu, L. Messing, D. Balschun, R. D'Hooge and E. M. Mandelkow (2012). "Cognitive defects are reversible in inducible mice expressing pro-aggregant full-length human Tau." Acta Neuropathol. **123**(6): 787-805.
von Bergen, M., S. Barghorn, J. Biernat, E. M. Mandelkow and E. Mandelkow (2005). "Tau aggregation is driven by a transition from random coil to beta sheet structure." Biochim Biophys Acta **1739**(2-3): 158-166.
Wang, Y. and E. Mandelkow (2015). "Tau in physiology and pathology." Nat Rev Neurosci **17**(1): 5-21.
Wischik, C., P. Edwards, R. Lai, M. Roth and C. Harrington (1996). "Selective inhibition of Alzheimer disease-like tau aggregation by phenothiazines." Proc Natl Acad Sci U S A **93**(20): 11213-11218.
Wischik, C., R. Staff, D. Wischik, P. Bentham, A. Murray, J. Storey, K. Kook and C. Harrington (2015). "Tau aggregation inhibitor therapy: an exploratory phase 2 study in mild or moderate Alzheimer's disease." J Alzheimers Dis. **44**(2): 705-720.
Wittmann, C. W., M. F. Wszolek, J. M. Shulman, P. M. Salvaterra, J. Lewis, M. Hutton and M. B. Feany (2001). "Tauopathy in Drosophila: neurodegeneration without neurofibrillary tangles." Science **293**(5530): 711-714.
Zhang, Y., K.-M. Wu, L. Yang, Q. Dong and J.-T. Yu (2022). "Tauopathies: New perspectives and challenges " Molecular Neurodegeneration **17**: 28.

FIGURES & LEGENDS

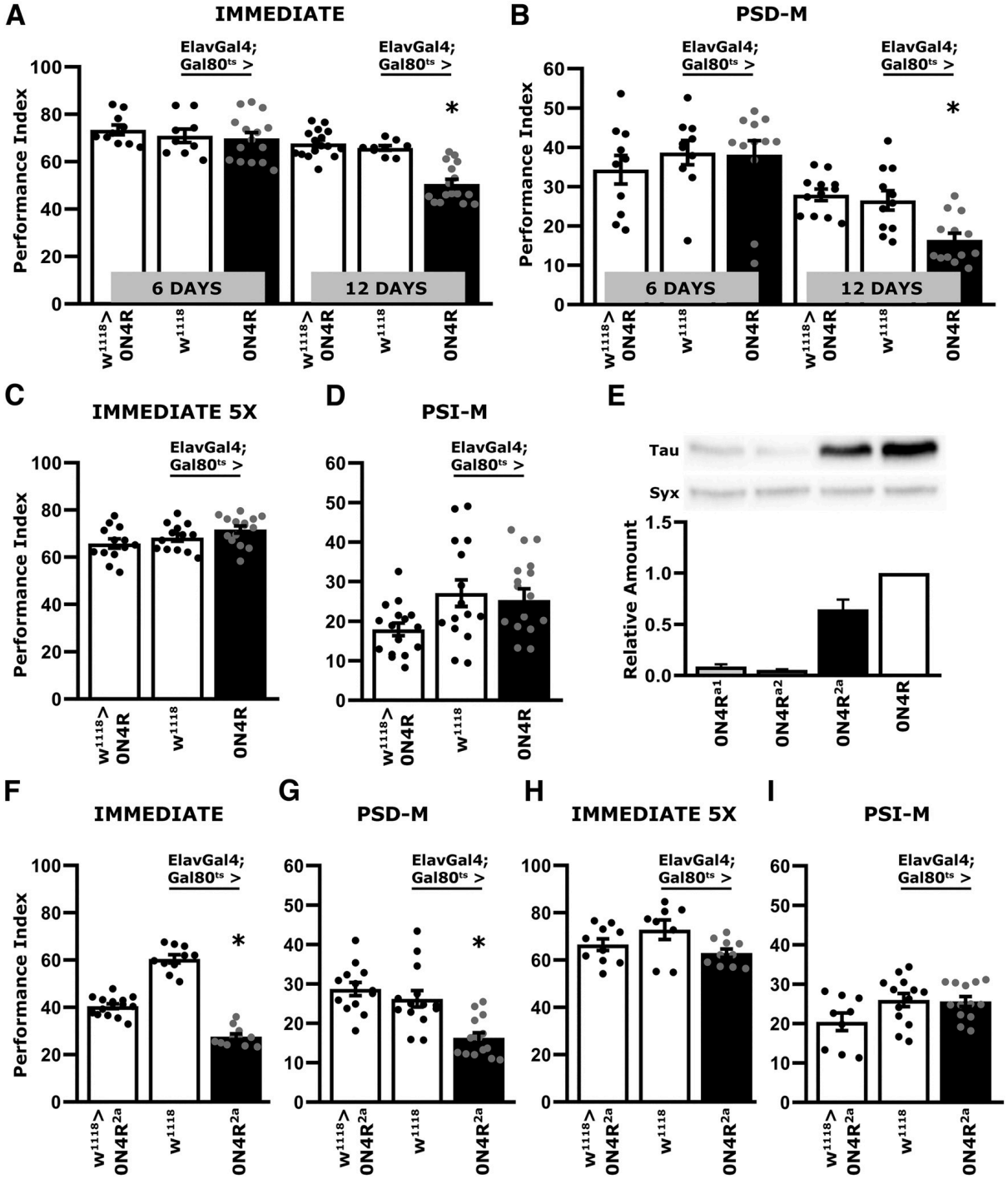

Figure 1. Deficient associative learning and PSD-M emerge in a time-dependent manner upon hTau^{0N4R} expression in the adult CNS.

Bars represent the mean performance indexes (PI) and standard errors of the mean (± S.E.M.) for the number of indicated experimental replicates (n). Stars indicate significant differences. All statistical details are presented in the Statistics Table. Black Bars represent the experimental strains and open bars the controls as indicated.

A) Immediate Performance after one round of standard conditioning (Learning) and 24hr Spaced Conditioning memory (PSD-M) performance of animals accumulating pan-neuronally the $hTau^{0N4R}$ isoform for 6 and 12 days compared to that of driver and transgene heterozygotes. $n \geq 12$ for all genotypes.

B) 24hr Spaced Conditioning memory (PSD-M) performance of animals accumulating pan-neuronally $hTau^{0N4R}$ for 6 and 12 days compared to that of driver and transgene heterozygotes. $n \geq 11$ for all genotypes.

C) Immediate Performance after Extended Conditioning (5X) of flies accumulating pan-neuronally $hTau^{0N4R}$ for 12 days compared to that of driver and transgene heterozygotes. $n \geq 12$ for all genotypes.

D) 24hr Massed Conditioning (PSI-M) memory of flies accumulating pan-neuronally $hTau^{0N4R}$ for 12 days compared to that of driver and transgene heterozygotes. $n \geq 12$ for all genotypes

E) Representative Western blots from head lysates of flies pan-neuronally accumulating $hTau^{0N4R}$ for 12 days compared with similar lysates from $hTau^{0N4Ra1}$, $hTau^{0N4Ra2}$ and the double transgenic strain $hTau^{0N4R2a}$, probed with the 5A6 anti-Tau antibody. Syntaxin (Syx) levels in the lysates were used as quantification normalizer. Tau levels were normalized using the Syx loading control and are shown as a ratio of their mean ± SEM values relative to respective levels in flies accumulating $hTau^{0N4R}$, which was set to 1. $n \geq 4$ for all genotypes

F) Performance immediately after one round of standard conditioning (Learning) animals accumulating pan-neuronally $hTau^{0N4R}$ from the double transgenic $hTau^{0N4R2a}$ strain for 12 days and heterozygous controls. $n \geq 12$ for all genotypes.

G) 24hr Spaced Conditioning memory (PSD-M) performance of animals accumulating pan-neuronally $hTau^{0N4R}$ from the double transgenic $hTau^{0N4R2a}$ for 12 days and heterozygous controls. $n \geq 13$ for all genotypes.

H) Immediate Performance after Extended Conditioning (5X) of flies accumulating pan-neuronally $hTau^{0N4R}$ from the double transgenic $hTau^{0N4R2a}$ strain for 12 days and heterozygous controls. $n \geq 9$ for all genotypes.

I) 24hr Massed Conditioning (PSI-M) memory of flies accumulating pan-neuronally $hTau^{0N4R}$ from the double transgenic $hTau^{0N4R2a}$ for 12 days and heterozygous controls. $n \geq 11$ for all genotypes.

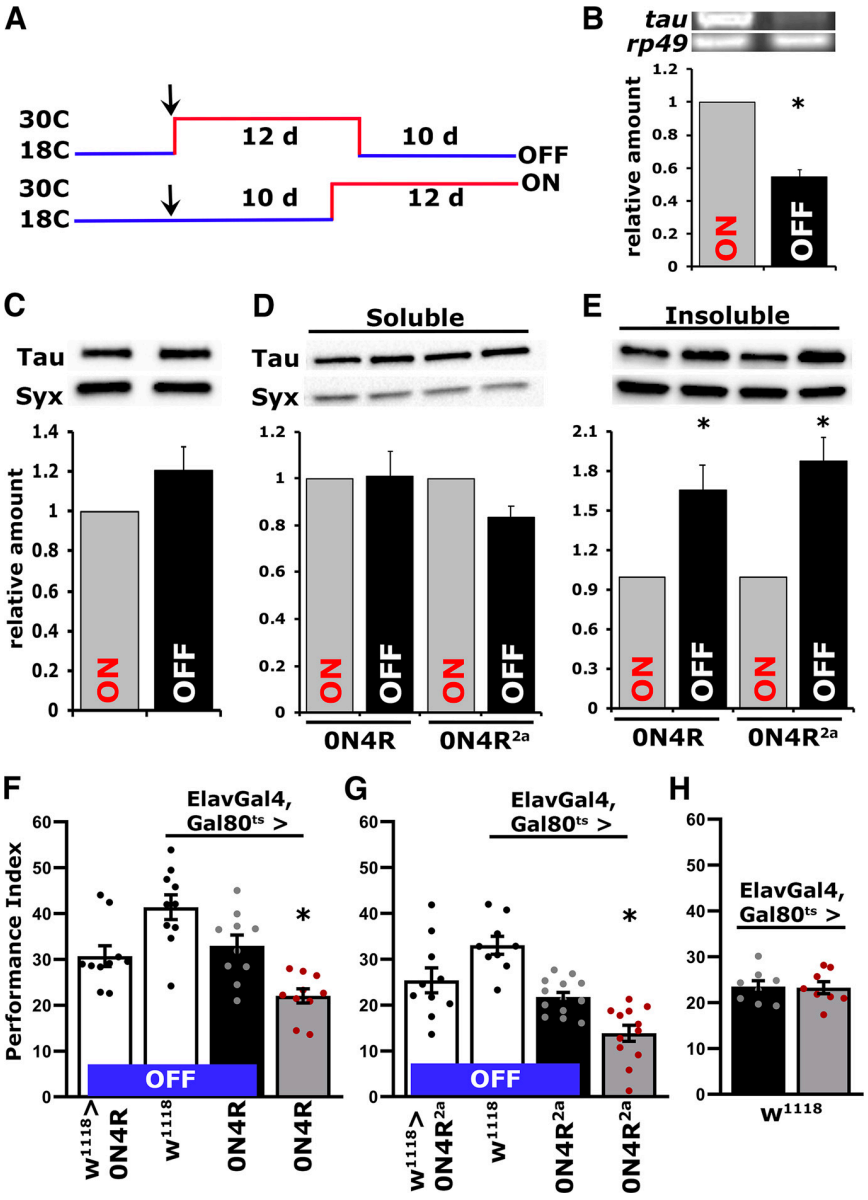

Figure 2. Reversal of the PSD-M deficit is correlated with Tau insoluble aggregate accumulation.

A) A schematic of the hTau^{0N4R} transgene repression (OFF) and expression protocol conditions (ON). The two groups of genotypically identical and of similar age animals hTau^{0N4R} is either repressed for 10 days of maintaining the flies at 18°C, following 12 days of expression (OFF), or is expressed for 12 days at 30°C (ON) after maintaining the adults flies for 10 days at 18°C.

B) Representative RT-PCR of Tau mRNA levels in flies with either repressed (OFF) or pan-neuronally expressing hTau^{0N4R} (ON). The *rp49* RNA levels served as internal reference and as a normalization control for the quantifications. The normalized level of hTau^{0N4R} (ON) for each quantification was fixed to 1. Error bars indicate mean ± SEM relative mRNA levels at the OFF condition relative to that of the ON condition. The star indicates significant differences from the control. n=7 determinations for both conditions.

C) Representative Western blots from head lysates of flies accumulating $hTau^{0N4R}$ pan-neuronally for 12 days (ON) compared with similar lysates from flies with $hTau^{0N4R}$ transgene repression (OFF) probed with the 5A6 anti-Tau antibody. The level of syntaxin (Syx) in the lysates was used as control for quantifications. For the quantification, Tau levels were normalized using the Syx loading control and are shown as a ratio of their mean ± SEM values relative to the respective levels under ON conditions. n=6 independent blots for both conditions.

D) Representative Western blot of soluble fractions of head lysates under expression (ON), or repression (OFF) conditions probed with the 5A6 anti-Tau antibody. The level of syntaxin (Syx) was used as control for quantifications. Tau levels were normalized using the Syx loading control and are shown as a ratio of their mean ± SEM relative to respective levels in flies accumulating pan-neuronally $hTau^{0N4R}$ or $hTau^{0N4R2a}$ for 12 days, which were set to 1. The stars indicate significant differences from the control genotype. $n \geq 5$ for $hTau^{0N4R}$ and $n \geq 6$ for $hTau^{0N4R2a}$ n=6 independent blots.

E) Representative Western blot of insoluble fractions of head lysates under expression (ON), or repression (OFF) conditions probed with the 5A6 anti-Tau antibody. Tau levels were normalized using the Syx loading control and are shown as a ratio of their mean ± SEM relative to respective levels in flies accumulating pan-neuronally $hTau^{0N4R}$ or $hTau^{0N4R2a}$ for 12 days, which were set to 1. The stars indicate significant differences from the control genotype. $n \geq 5$ for $hTau^{0N4R}$ and $n \geq 4$ for $hTau^{0N4R2a}$ independent blots.

F-G) Bars represent the mean performance indexes (PI) and standard errors of the mean (± S.E.M.) for the number of indicated experimental replicates (n). Stars indicate significant differences. 24hr Spaced Conditioning memory (PSD-M) performance of animals accumulating pan-neuronally $hTau^{0N4R}$ (F) or $hTau^{0N4R2a}$ (G) for 12 days at 30°C (ON, grey bars) compared with driver and transgene heterozygotes (open bars) and animals with repressed transgenes (Black bars). $n \geq 9$ for F and $n \geq 10$ for G.

H) Mean performance indexes (PI) and standard errors of the mean (± S.E.M.) for 24hr Spaced Conditioning memory (PSD-M) performance of control animals kept either for 12 days at 30°C (gray bar) after 10 days as adults at 18°C, or 10 days at 18°C following 12 days at 30°C (black bar). n=8 for both groups.

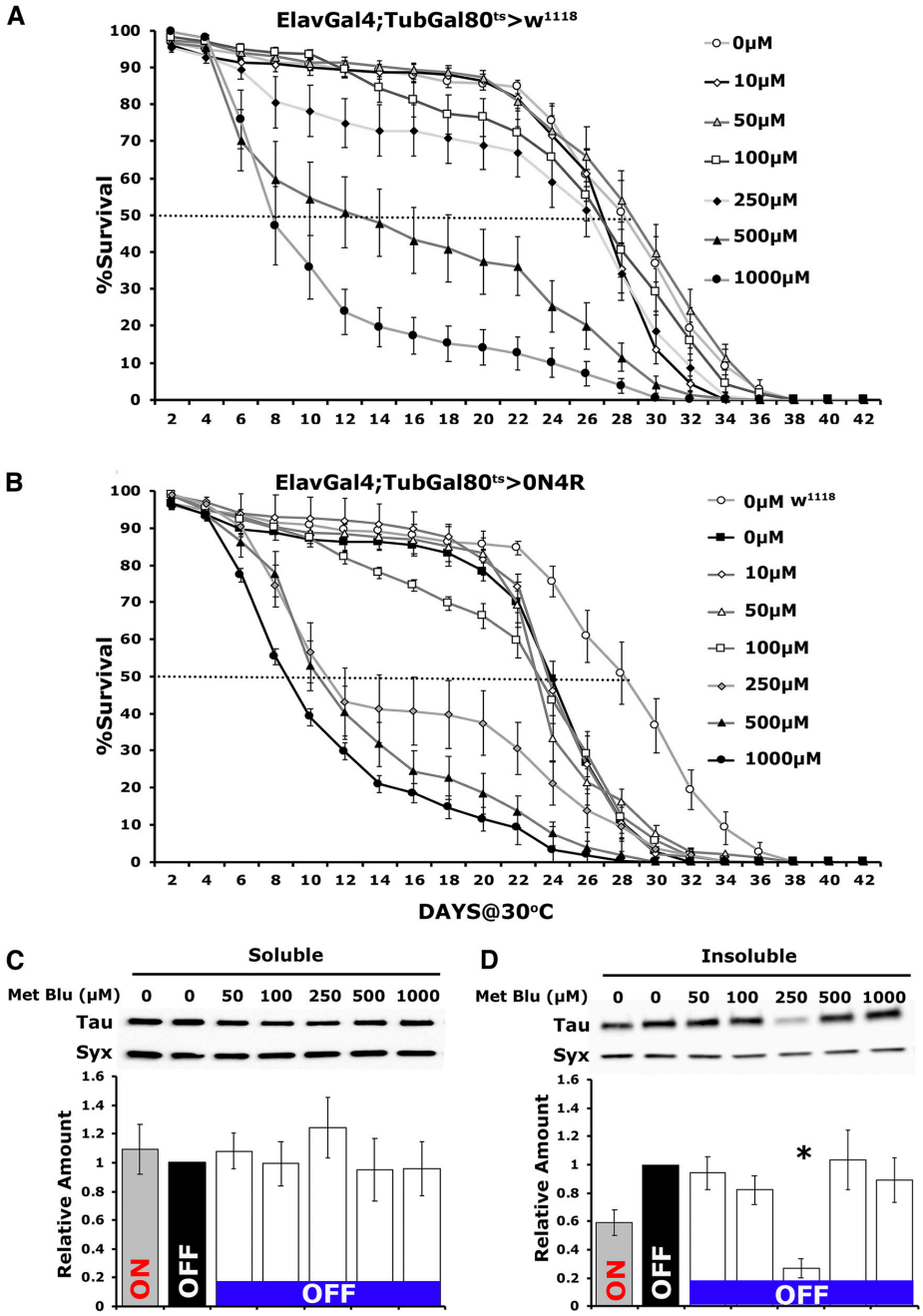

Figure 3. Methylene Blue prevents insoluble hTau^{0N4R} aggregate formation at a specific concentration.

A, B) Survival curves of untreated and treated with different concentrations of MetBlu driver heterozygote control (A) and animals accumulating pan-neuronally hTau^{0N4R} at 30°C (B). The data represent the mean ± SEM from two independent experiments with at least 300 flies assessed per genotype. The different concentrations of MetBlu are indicated on the right. The dotted lines indicate the 50% attrition levels. Statistical details in Table 1 and 2 respectively.

C, D) Representative Western blots of soluble (C) and insoluble (D) fractions generated from adult flies untreated or treated with different concentrations of MetBlu probed with 5A6 anti-Tau antibody.

hTau^{0N4R} was either expressed for 12 days (ON) or is repressed for 10 days following 12 days of expression (OFF). To determine the effect of the drug on hTau^{0N4R} insoluble aggregate formation, flies were shifted onto food containing MetBlu ranging from 50 to 1000 µM at 18^{o}C to silence the transgene for 10 days (OFF). The different concentrations of MetBlu used are indicated above each bar. The level of syntaxin (Syx) was used as control for quantifications. The normalized level of hTau^{0N4R} (OFF condition, untreated) for each quantification was fixed to 1. Error bars indicate mean ± SEM relative to respective levels in flies that exist under transgene transcriptional silencing conditions. The star indicates significant differences from the control genotype. n≥ 5 for C and n≥ 6 independent blots.

Wilkoxon/Kruscal-Wallis			Means comparison (Steel with control)		
DAY	**χ^2, (DF, count)**	$p>\chi^2$	**Genotype (µM MetBlu)**	**z**	**p**
2	17.015 (6,17)	**0.0092**	Elav;G80^{ts}> + **0**		
			Elav;G80^{ts}> + **10**		
			Elav;G80^{ts}> + **50**		
			Elav;G80^{ts}> + **100**		
			Elav;G80^{ts}> + **250**		
			Elav;G80^{ts}> + **500**	0.4029	0.9975
			Elav;G80^{ts}> + **1000**	2.9594	0.0161
6	8.044 (6,17)	0.2349	Elav;G80^{ts}> + **0**		
			Elav;G80^{ts}> + **10**		
			Elav;G80^{ts}> + **50**		
			Elav;G80^{ts}> + **100**		
			Elav;G80^{ts}> + **250**		
			Elav;G80^{ts}> + **500**		
			Elav;G80^{ts}> + **1000**		
10	44.54 (6,17)	**<0.0001**	Elav;G80^{ts}> + **0**		
			Elav;G80^{ts}> + **10**		
			Elav;G80^{ts}> + **50**		
			Elav;G80^{ts}> + **100**		
			Elav;G80^{ts}> + **250**		
			Elav;G80^{ts}> + **500**	-2.9765	0.0153
			Elav;G80^{ts}> + **1000**	-4.9758	**<0.0001**
14	60.578 (6,17)	**<0.0001**	Elav;G80^{ts}> + **0**		
			Elav;G80^{ts}> + **10**		
			Elav;G80^{ts}> + **50**		
			Elav;G80^{ts}> + **100**		
			Elav;G80^{ts}> + **250**	-2,6753	0.0372
			Elav;G80^{ts}> + **500**	-3.8591	**0.0007**
			Elav;G80^{ts}> + **1000**	-4.9943	**<0.0001**
18	63.859 (6,17)	**<0.0001**	Elav;G80^{ts}> + **0**		
			Elav;G80^{ts}> + **10**		
			Elav;G80^{ts}> + **50**		
			Elav;G80^{ts}> + **100**		
			Elav;G80^{ts}> + **250**	-2.4139	0.075
			Elav;G80^{ts}> + **500**	-4.2418	**0.0001**
			Elav;G80^{ts}> + **1000**	-5.0056	**<0.0001**
22	58,397 (6,17)	**<0.0001**	Elav;G80^{ts}> + **0**		
			Elav;G80^{ts}> + **10**		
			Elav;G80^{ts}> + **50**		
			Elav;G80^{ts}> + **100**		
			Elav;G80^{ts}> + **250**	-1.8873	0.2439
			Elav;G80^{ts}> + **500**	-4.3894	**<0.0001**
			Elav;G80^{ts}> + **1000**	-4.9321	**<0.0001**
26	43.698 (6,17)	**<0.0001**	Elav;G80^{ts}> + **0**		
			Elav;G80^{ts}> + **10**		
			Elav;G80^{ts}> + **50**		
			Elav;G80^{ts}> + **100**		
			Elav;G80^{ts}> + **250**	-1.0555	0.7870
			Elav;G80^{ts}> + **500**	-3.4394	**0.0032**
			Elav;G80^{ts}> + **1000**	-4.4177	**<0.0001**
30	39.271 (6,17)	**<0.0001**	Elav;G80^{ts}> + **0**		

			Elav;G80^{ts}> + **10**	-2.1832	0.3149
			Elav;G80^{ts}> + **50**		
			Elav;G80^{ts}> + **100**		
			Elav;G80^{ts}> + **250**	-2.1833	0.1287
			Elav;G80^{ts}> + **500**	-36036	**0.0018**
			Elav;G80^{ts}> + **1000**	-4.1500	**0.0002**
34	26.7302 (6,17)	**0.0002**	Elav;G80^{ts}> + **0**		
			Elav;G80^{ts}> + **10**	-2.6180	0.0436
			Elav;G80^{ts}> + **50**		
			Elav;G80^{ts}> + **100**		
			Elav;G80^{ts}> + **250**	-2.0723	0.1642
			Elav;G80^{ts}> + **500**	-2.1460	0.1398
			Elav;G80^{ts}> + **1000**	-2.6181	0.0436
38	0.0000 (6,17)	1.0000	Elav;G80^{ts}> + **0**		
			Elav;G80^{ts}> + **10**		
			Elav;G80^{ts}> + **50**		
			Elav;G80^{ts}> + **100**		
			Elav;G80^{ts}> + **250**		
			Elav;G80^{ts}> + **500**		
			Elav;G80^{ts}> + **1000**		

Table 1. Survival statistics for control heterozygotes kept on the indicated concentrations of MetBlu at 30ºC.

Survival results from all the independent determinations were compared with Wilcoxon/Kruskal-Wallis tests for the indicated days. If a positive (χ^2) outcome, the means from each genotype for the days with significant differences were compared using the Steel with control tests whose z ratio and p values are shown. Significant differences from controls are emphasized with bold.

Wilkoxon/Kruscal-Wallis			Means comparison (Steel with control)		
DAY	**χ^2, (DF, count)**	$p>\chi^2$	**Genotype (µM MetBlu)**	**z**	**p**
2	13.5961 (6,17)	0.0834	Elav;G80^{ts}> 0N4R **0**		
			Elav;G80^{ts}> 0N4R **10**		
			Elav;G80^{ts}> 0N4R **50**		
			Elav;G80^{ts}> 0N4R **100**		
			Elav;G80^{ts}> 0N4R **250**		
			Elav;G80^{ts}> 0N4R **500**		
			Elav;G80^{ts}> 0N4R **1000**		
6	18.4831 (6,17)	**0.0051**	Elav;G80^{ts}> 0N4R **0**		
			Elav;G80^{ts}> 0N4R **10**		
			Elav;G80^{ts}> 0N4R **50**		
			Elav;G80^{ts}> 0N4R **100**		
			Elav;G80^{ts}> 0N4R **250**		
			Elav;G80^{ts}> 0N4R **500**		
			Elav;G80^{ts}> 0N4R **1000**	-2.1034	0.1536
10	65.901 (6,17)	**<0.0001**	Elav;G80^{ts}> 0N4R **0**		
			Elav;G80^{ts}> 0N4R **10**		
			Elav;G80^{ts}> 0N4R **50**		
			Elav;G80^{ts}> 0N4R **100**		
			Elav;G80^{ts}> 0N4R **250**	-3.0928	0.0106
			Elav;G80^{ts}> 0N4R **500**	-3.8612	**0.0006**
			Elav;G80^{ts}> 0N4R **1000**	-4.8594	**<0.0001**
14	76.510 (6,17)	**<0.0001**	Elav;G80^{ts}> 0N4R **0**		
			Elav;G80^{ts}> 0N4R **10**		
			Elav;G80^{ts}> 0N4R **50**		
			Elav;G80^{ts}> 0N4R **100**	-1.7623	0.3028
			Elav;G80^{ts}> 0N4R **250**	-3.7252	**0.0011**
			Elav;G80^{ts}> 0N4R **500**	-4.9123	**<0.0001**
			Elav;G80^{ts}> 0N4R **1000**	-4.8496	**<0.0001**
18	73.901 (6,17)	**<0.0001**	Elav;G80^{ts}> 0N4R **0**		
			Elav;G80^{ts}> 0N4R **10**		
			Elav;G80^{ts}> 0N4R **50**		
			Elav;G80^{ts}> 0N4R **100**	-1.5947	0.4017
			Elav;G80^{ts}> 0N4R **250**	-3.4581	**0.0030**
			Elav;G80^{ts}> 0N4R **500**	-4.8533	**<0.0001**
			Elav;G80^{ts}> 0N4R **1000**	-4.9939	**<0.0001**
22	70.196 (6,17)	**<0.0001**	Elav;G80^{ts}> 0N4R **0**		
			Elav;G80^{ts}> 0N4R **10**		
			Elav;G80^{ts}> 0N4R **50**		
			Elav;G80^{ts}> 0N4R **100**	-0.7294	0.9497
			Elav;G80^{ts}> 0N4R **250**	-3.6844	**0.0013**
			Elav;G80^{ts}> 0N4R **500**	-4.8786	**<0.0001**
			Elav;G80^{ts}> 0N4R **1000**	-4.9903	**<0.0001**
26	30.019 (6,17)	**<0.0001**	Elav;G80^{ts}> 0N4R **0**		
			Elav;G80^{ts}> 0N4R **10**		
			Elav;G80^{ts}> 0N4R **50**		
			Elav;G80^{ts}> 0N4R **100**		
			Elav;G80^{ts}> 0N4R **250**	-1.5003	0.4648
			Elav;G80^{ts}> 0N4R **500**	-2.9561	**0.0163**
			Elav;G80^{ts}> 0N4R **1000**	-3.6461	**0.0015**

30	15.404 (6,17)	0.0173	Elav;G80^{ts}> 0N4R **0**		
			Elav;G80^{ts}> 0N4R **10**		
			Elav;G80^{ts}> 0N4R **50**		
			Elav;G80^{ts}> 0N4R **100**		
			Elav;G80^{ts}> 0N4R **250**	-0.9155	0.8626
			Elav;G80^{ts}> 0N4R **500**	-2.2021	0.1204
			Elav;G80^{ts}> 0N4R **1000**	-2.2018	0.1204
34	5.1170 (6,17)	0.5289	Elav;G80^{ts}> 0N4R **0**		
			Elav;G80^{ts}> 0N4R **10**		
			Elav;G80^{ts}> 0N4R **50**		
			Elav;G80^{ts}> 0N4R **100**		
			Elav;G80^{ts}> 0N4R **250**		
			Elav;G80^{ts}> 0N4R **500**		
			Elav;G80^{ts}> 0N4R **1000**		
38	0.0000 (6,17)	1.0000	Elav;G80^{ts}> 0N4R **0**		
			Elav;G80^{ts}> 0N4R **10**		
			Elav;G80^{ts}> 0N4R **50**		
			Elav;G80^{ts}> 0N4R **100**		
			Elav;G80^{ts}> 0N4R **250**		
			Elav;G80^{ts}> 0N4R **500**		
			Elav;G80^{ts}> 0N4R **1000**		
			Elav;G80^{ts}> 0N4R **1000**		

Table 2. Survival statistics for flies expressing hTau^{0N4R} kept on the indicated concentrations of MetBlu at 30^{o}C.

Survival results from all the independent determinations were compared with Wilcoxon/Kruskal-Wallis tests for the indicated days. If a positive (χ^2) outcome, the means from each genotype for the days with significant differences were compared using the Steel with control tests whose z ratio and p values are shown. Significant differences from controls are emphasized with bold.

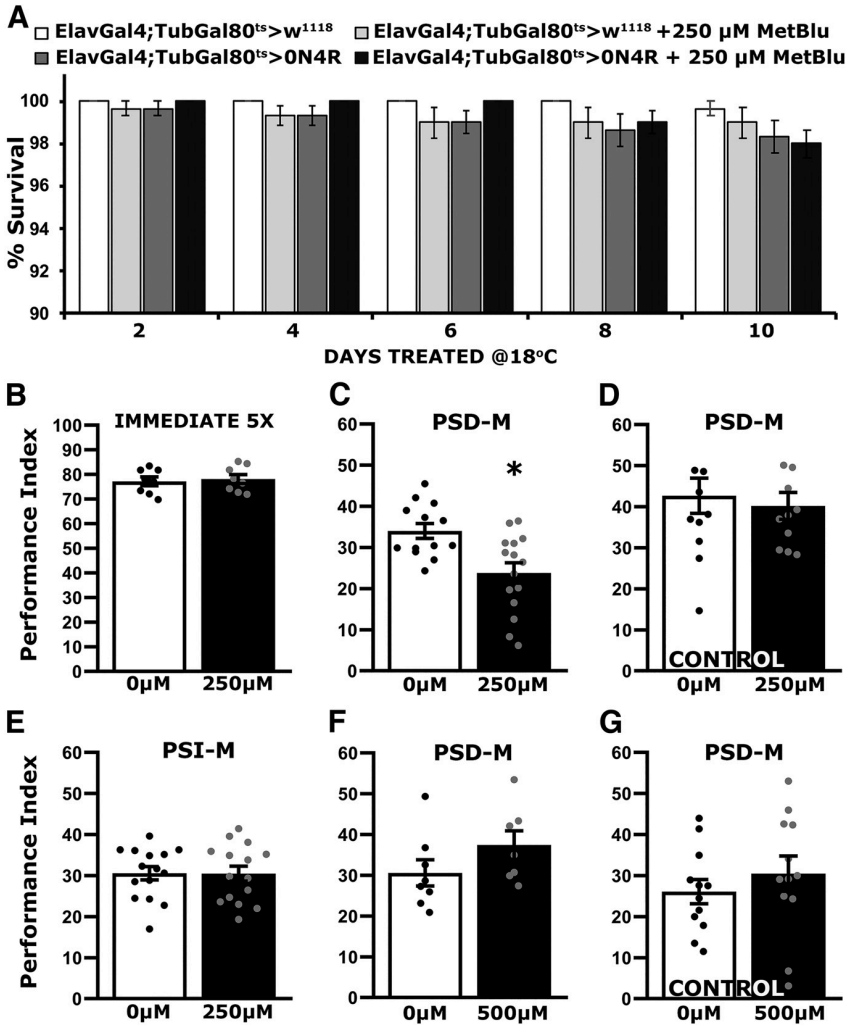

Figure 4. Preventing hTau^{0N4R} insoluble aggregate formation results in defective PSD-M under transgene transcriptional silencing conditions.

A) Survival histogram for hTau^{0N4R} animals kept under transgene silencing conditions (OFF, 18°C), but on MetBlu for 10 days compared with driver heterozygotes. The survival rates were over 98% in these conditions for all genotypes independent of drug administration. The data represent the mean ± SEM from two independent experiments with at least 300 flies assessed per genotype.

B-G) Bars represent the mean performance indexes (PI) and standard errors of the mean (± S.E.M.) for the number of indicated experimental replicates (n). Stars indicate significant differences.

B) Immediate Performance after Extended Conditioning (5X) of hTau^{0N4R}-expressing flies kept for 10 days in the OFF condition in the absence (0µM) or presence of 250µM MetBlu. n≥ 7 per condition.

C) 24hr Spaced Conditioning memory (PSD-M) performance of hTau^{0N4R}-expressing flies kept for 10 days in the OFF condition in the absence (0µM) or presence of 250µM MetBlu. n≥ 13 per condition.

D) 24hr Spaced Conditioning memory (PSD-M) performance of control animals kept for 10 days in the OFF condition in the absence (0µM) or presence of 250µM MetBlu. n≥ 11 per condition.

E) 24hr Massed Conditioning (PSI-M) memory of hTau^{0N4R}-expressing flies kept for 10 days in the OFF condition in the absence (0µM) or presence of 250µM MetBlu. n≥ 14 per condition.

F) 24hr Spaced Conditioning memory (PSD-M) performance of hTau^{0N4R}-expressing flies kept for 10 days in the OFF condition in the absence (0µM) or presence of 500µM MetBlu. n≥ 7 per condition.

G) 24hr Spaced Conditioning memory (PSD-M) performance of control animals kept for 10 days in the OFF condition in the absence (0µM) or presence of 500µM MetBlu. n=12 per condition.

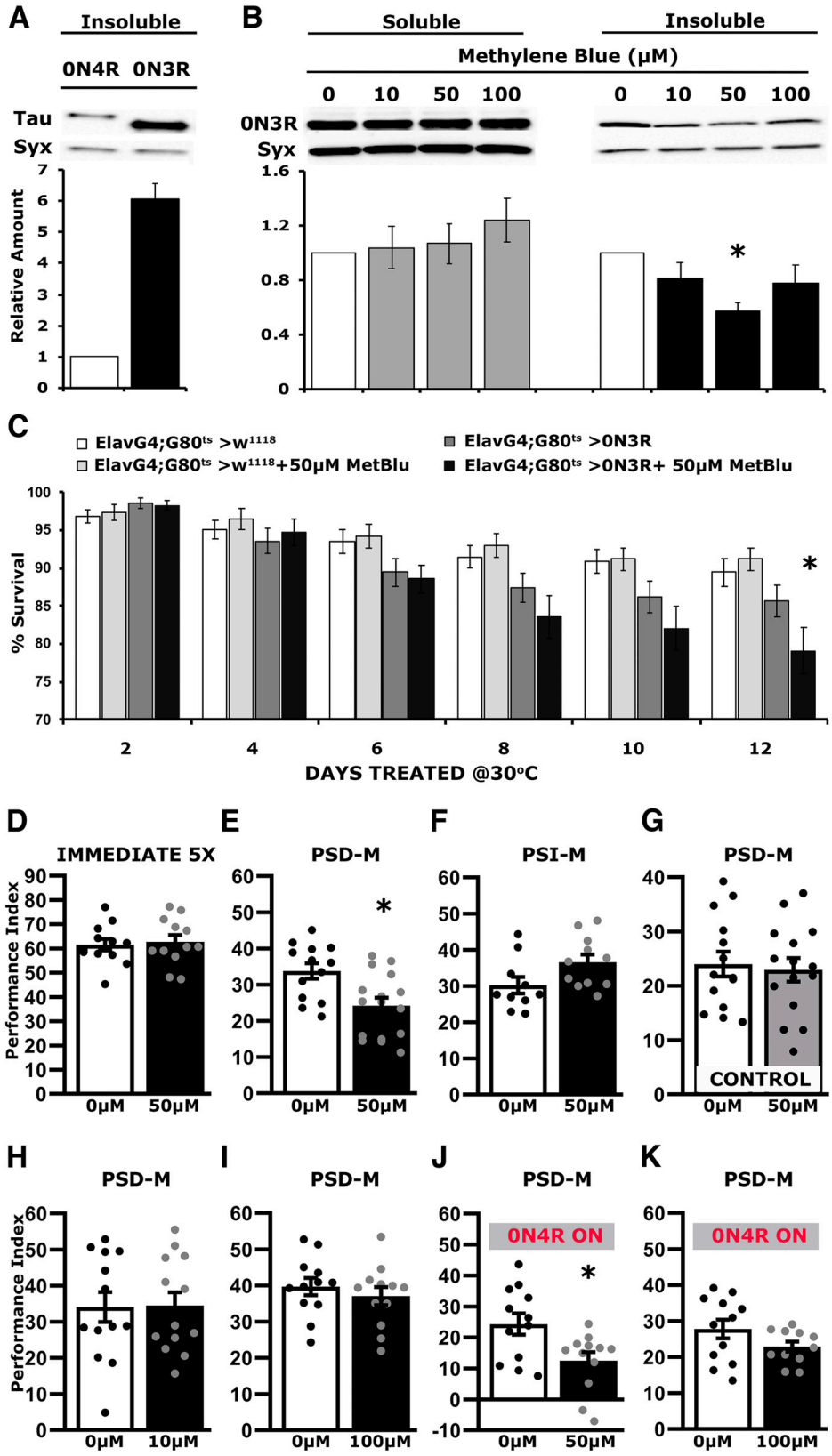

Figure 5. Blocking hTau^{0N3R} insoluble aggregate formation results in defective PSD-M.

A) Representative western blots of insoluble fractions generated from adult heads, following pan-neuronal expression of hTau^{0N4R} and hTau^{0N3R} transgenes for 12days at 30°C, probed with the 5A6 anti-Tau antibody. The level of syntaxin (Syx) was used as control for quantifications. The normalized level

of hTau^{0N4R} for each quantification was fixed to 1. Error bars indicate mean ± SEM of insoluble hTau levels in flies that express hTau^{0N3R}over that of the hTau^{0N4R}. The star indicates significant differences from that in hTau^{0N4R}-expressing lysates. n≥ 4 independent blots.

B) Representative western blots of soluble and insoluble fractions generated from adult heads, following pan-neuronal hTau^{0N3R} expression for 12days at 30^{o}C in flies kept on different concentrations of MetBlu (0, 10, 50 and 100µM), as indicated probed with the 5A6 antibody., The level of syntaxin (Syx) was used as loading control. For the quantification, Tau levels were normalized using the Syx loading control and are shown as a ratio of their mean ± SEM values relative to respective levels in untreated flies accumulating hTau^{0N3R}, which were set to 1. The star indicates significant differences from the untreated with MetBlu animals. n≥ 4 for soluble and n>12 for Insoluble independent blots.

C) Survival histogram of animals of the indicated genotype untreated or treated with 50µM MetBlu at 30^{o}C compared with driver heterozygotes. MetBlu at 50µM did not affect survival of driver heterozygotes. The data represent the mean ± SEM from two independent experiments with at least 300 flies assessed per genotype. Statistical details in the statistics table. The star indicates significant differences form the control genotype on the respective day.

D-K) Bars represent the mean performance indexes (PI) and standard errors of the mean (± S.E.M.) for the number of indicated experimental replicates (n). Stars indicate significant differences.

D) Immediate Performance after Extended Conditioning (5X) of hTau^{0N3R}-expressing flies kept for 12 days in the ON condition in the absence (0µM) or presence of 50µM MetBlu. n≥ 11 per condition.

E) 24hr Spaced Conditioning memory (PSD-M) performance of hTau^{0N3R}-expressing flies kept for 12 days in the ON condition in the absence (0µM) or presence of 50µM MetBlu. n≥ 14 per condition.

F) 24hr Massed Conditioning (PSI-M) memory of hTau^{0N3R}-expressing flies kept for 12 days in the ON condition in the absence (0µM) or presence of 50µM MetBlu. n≥10 per condition.

G) 24hr Spaced Conditioning memory (PSD-M) performance of control animals kept for 12 days in the ON condition in the absence (0µM) or presence of 50µM MetBlu. n≥ 14 per condition.

H) 24hr Spaced Conditioning memory (PSD-M) performance of hTau^{0N3R}-expressing flies kept for 12 days in the ON condition in the absence (0µM) or presence of 10µM MetBlu. n≥ 13 per condition.

I) 24hr Spaced Conditioning memory (PSD-M) performance of hTau^{0N3R}-expressing flies kept for 12 days in the ON condition in the absence (0µM) or presence of 100µM MetBlu. n≥ 12 per condition.

J) 24hr Spaced Conditioning memory (PSD-M) performance of hTau^{0N4R}-expressing flies kept for 12 days in the ON condition in the absence (0µM) or presence of 50µM MetBlu. n=12 per condition.

K) 24hr Spaced Conditioning memory (PSD-M) performance of hTau^{0N4R}-expressing flies kept for 12 days in the ON condition in the absence (0µM) or presence of 100µM MetBlu. n≥ 11 per condition.

Wilkoxon/Kruscal-Wallis			Means comparison (Steel with control)		
DAY	**χ^2, (DF, count)**	**p>χ^2**	**Genotype (µM MetBlu)**	**z**	**p**
2	14,6455 (6,17)	0.0232	Elav;G80^{ts}> 0N3R **0**		
			Elav;G80^{ts}> 0N3R **10**		
			Elav;G80^{ts}> 0N3R **50**		
			Elav;G80^{ts}> 0N3R **100**	-0.6696	0.9657
			Elav;G80^{ts}> 0N3R **250**	-2.5453	0.0530
			Elav;G80^{ts}> 0N3R **500**		
			Elav;G80^{ts}> 0N3R **1000**		
6	83,7625 (6,17)	**<0.0001**	Elav;G80^{ts}> 0N3R **0**		
			Elav;G80^{ts}> 0N3R **10**		
			Elav;G80^{ts}> 0N3R **50**		
			Elav;G80^{ts}> 0N3R **100**	-0.7908	0.9280
			Elav;G80^{ts}> 0N3R **250**	-4.5530	**<0.0001**
			Elav;G80^{ts}> 0N3R **500**	-4.6673	**<0.0001**
			Elav;G80^{ts}> 0N3R **1000**	-4.9777	**<0.0001**
10	99.929 (6,17)	**<0.0001**	Elav;G80^{ts}> 0N3R **0**		
			Elav;G80^{ts}> 0N3R **10**		
			Elav;G80^{ts}> 0N3R **50**	-0.8090	0.9208
			Elav;G80^{ts}> 0N3R **100**	-3.9799	**0.0004**
			Elav;G80^{ts}> 0N3R **250**	-5.1601	**<0.0001**
			Elav;G80^{ts}> 0N3R **500**	-5.2584	**<0.0001**
			Elav;G80^{ts}> 0N3R **1000**	-5.2050	**<0.0001**
14	104.714 (6,17)	**<0.0001**	Elav;G80^{ts}> 0N3R **0**		
			Elav;G80^{ts}> 0N3R **10**	0.2637	0.9998
			Elav;G80^{ts}> 0N3R **50**	-3.1629	**0.0084**
			Elav;G80^{ts}> 0N3R **100**	-4.9986	**<0.0001**
			Elav;G80^{ts}> 0N3R **250**	-5.3209	**<0.0001**
			Elav;G80^{ts}> 0N3R **500**	-5.2584	**<0.0001**
			Elav;G80^{ts}> 0N3R **1000**	-5.3209	**<0.0001**
18	108.364 (6,17)	**<0.0001**	Elav;G80^{ts}> 0N3R **0**		
			Elav;G80^{ts}> 0N3R **10**	-2.3846	0.0799
			Elav;G80^{ts}> 0N3R **50**	-4.9932	**<0.0001**
			Elav;G80^{ts}> 0N3R **100**	-5.1725	**<0.0001**
			Elav;G80^{ts}> 0N3R **250**	-5.3345	**<0.0001**
			Elav;G80^{ts}> 0N3R **500**	-5.2715	**<0.0001**
			Elav;G80^{ts}> 0N3R **1000**	-5.3345	**<0.0001**
22	90.179 (6,17)	**<0.0001**	Elav;G80^{ts}> 0N3R **0**		
			Elav;G80^{ts}> 0N3R **10**	-1.9251	0.2222
			Elav;G80^{ts}> 0N3R **50**	-3.7813	**0.0009**
			Elav;G80^{ts}> 0N3R **100**	-4.9195	**<0.0001**
			Elav;G80^{ts}> 0N3R **250**	-5.0693	**<0.0001**
			Elav;G80^{ts}> 0N3R **500**	-5.0693	**<0.0001**
			Elav;G80^{ts}> 0N3R **1000**	-5.0609	**<0.0001**
26	21.133 (6,17)	**0.0017**	Elav;G80^{ts}> 0N3R **0**		
			Elav;G80^{ts}> 0N3R **10**		
			Elav;G80^{ts}> 0N3R **50**		
			Elav;G80^{ts}> 0N3R **100**		
			Elav;G80^{ts}> 0N3R **250**		
			Elav;G80^{ts}> 0N3R **500**	-1.3926	0.5432
			Elav;G80^{ts}> 0N3R **1000**	-1.3926	0.5432

30	6.000 (6,17)	0.4232	Elav;G80^{ts}> 0N3R **0**		
			Elav;G80^{ts}> 0N3R **10**		
			Elav;G80^{ts}> 0N3R **50**		
			Elav;G80^{ts}> 0N3R **100**		
			Elav;G80^{ts}> 0N3R **250**		
			Elav;G80^{ts}> 0N3R **500**		
			Elav;G80^{ts}> 0N3R **1000**		
34	0.000 (6,17)	1.0000	Elav;G80^{ts}> 0N3R **0**		
			Elav;G80^{ts}> 0N3R **10**		
			Elav;G80^{ts}> 0N3R **50**		
			Elav;G80^{ts}> 0N3R **100**		
			Elav;G80^{ts}> 0N3R **250**		
			Elav;G80^{ts}> 0N3R **500**		
			Elav;G80^{ts}> 0N3R **1000**		
38	0.000 (6,17)	1.0000	Elav;G80^{ts}> 0N3R **0**		
			Elav;G80^{ts}> 0N3R **10**		
			Elav;G80^{ts}> 0N3R **50**		
			Elav;G80^{ts}> 0N3R **100**		
			Elav;G80^{ts}> 0N3R **250**		
			Elav;G80^{ts}> 0N3R **500**		
			Elav;G80^{ts}> 0N3R **1000**		

Table 3. Survival statistics for flies expressing hTau^{0N3R} kept on the indicated concentrations of MetBlu at 30^{o}C.

Survival results from all the independent determinations were compared with Wilcoxon/Kruskal-Wallis tests for the indicated days. If a positive (χ^2) outcome, the means from each genotype for the days with significant differences were compared using the Steel with control tests whose z ratio and p values are shown. Significant differences from controls are emphasized with bold.

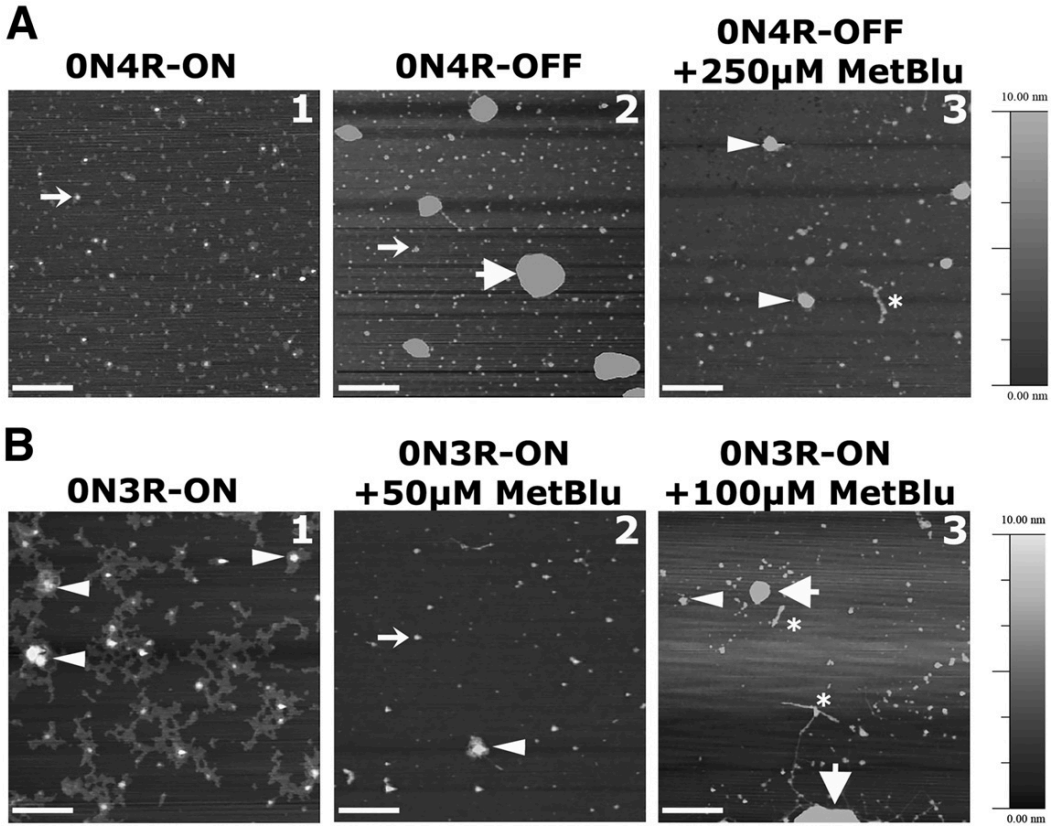

Figure 6. Aggregate accumulation in the CNS of hTau^{0N4R} and hTau^{0N3R}-expressing animals and MetBlu-mediated aggregate inhibition.

Representative AFM images of aggregates from insoluble Tau fractions in head lysates of hTau^{0N4R} and hTau^{0N3R}-expressing flies. The images were taken at random points from the mica carrying the indicated samples with a scan rate of 1Hz-2Hz. Scale bar 200nm.

A) Insoluble Tau fraction from adult pan-neuronally-expressing hTau^{0N4R} flies at the ON condition (**1**) or transgene repression conditions (**2**) and after treatment of repressed animals with 250μM MetBlu (**3**). Insoluble hTau under transgene repression were significantly elevated in number and size (**2**) compared to lysates from the ON condition (**1**). Treatment with 250μM MetBlu for 10 days at the OFF condition reduced the size and the number of aggregates, though short filaments appeared (**3**). Range of the filaments: <40 (thin arrow), 50-140nM (small arrowheads) to 240-390nm (thick arrow) and short filaments (asterisk).

B) Insoluble Tau fraction from adult pan-neuronally-expressing hTau^{0N3R} flies at the ON condition (**1**), the ON condition with simultaneous treatment with 50μM MetBlu (**2**) or 100μM MetBlu (**3**). Treatment with 50μM MetBlu for 12 days at 30^{o}C reduced the size of filaments, while treatment with 100μM MetBlu did not affect the size of the aggregates much, but yielded short filaments. Range of the aggregates: from 40-60nm (thin arrow), 80-150nm- (small arrowhead) >175nm (thick arrow) and short filaments (asterisk).

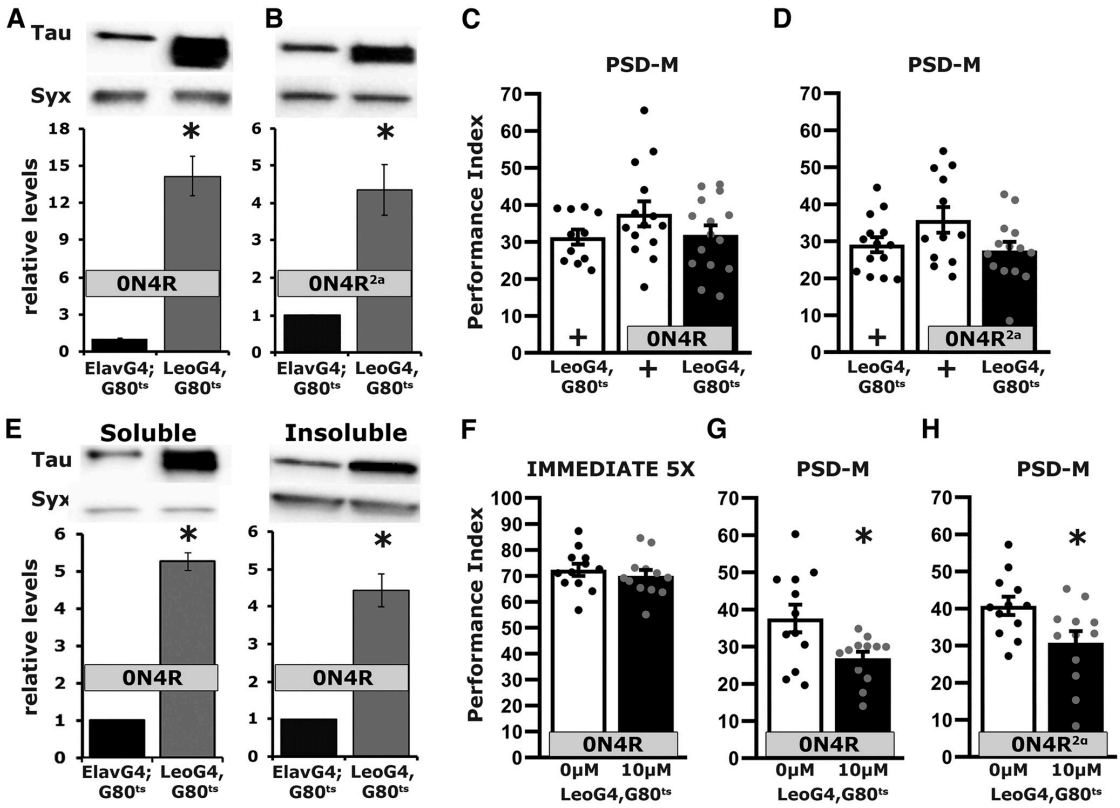

Figure 7. Insoluble aggregates in adult-specific hTau^{0N4R}-expressing animals within mushroom bodies are permissive to PSD-M.

A-B) Representative western blots from head lysates of flies accumulating hTau^{0N4R} pan-neuronally (ElavGal4; TubGal80^{ts}) for 12 days at 30^{o}C compared with flies expressing hTau^{0N4R} only in mushroom body neurons (LeoGal4; TubGal80^{ts}), probed with the 5A6 anti-Tau antibody. The level of syntaxin (Syx) in the lysates was used as control for quantifications. For the quantification, Tau levels were normalized using the Syx loading control and are shown as a ratio of their mean ± SEM values relative to respective levels in flies accumulating pan-neuronally the 0N4R isoform for 12 days, which was set to 1. The stars indicate significant differences from the control genotype. n≥ 5 per genotype in A and B.

C-D) Bars represent the mean performance indexes (PI) and standard errors of the mean (± S.E.M.) for the number of indicated experimental replicates (n). The genotypes of all animals are indicated below each bar.

C) 24hr Spaced Conditioning memory (PSD-M) performance of hTau^{0N4R}-expressing flies kept for 12 days in the ON condition. n≥ 13 per genotype

D) 24hr Spaced Conditioning memory (PSD-M) performance of hTau^{0N4R}-expressing flies from the hTau^{0N4R2a} double transgenics kept for 12 days in the ON condition. n≥ 13 per genotype.

E) Representative western blot of soluble (left) and insoluble (right) fractions generated from adult heads of flies accumulating $hTau^{0N4R}$ pan-neuronally or limited to mushroom body neurons for 12 days at 30°C, probed with the 5A6 anti-Tau antibody. Syntaxin (Syx) levels were used as control for quantifications. For the quantification, Tau levels were normalized using the Syx loading control and are shown as a ratio of their mean ± SEM values relative to respective levels in flies accumulating $hTau^{0N4R}$ pan-neuronally, which was set to 1. The mean ± SEM are shown for each group. The star indicates significant differences from the control genotype. $n \geq 5$ for both genotypes.

F-H) Bars represent the mean performance indexes (PI) and standard errors of the mean (± S.E.M.) for the number of indicated experimental replicates (n). Stars indicate significant differences.

F) Immediate Performance after Extended Conditioning (5X) of $hTau^{0N4R}$-expressing flies kept for 12 days in the ON condition in the absence (0µM) or presence of 10µM MetBlu. $n \geq 11$ per genotype.

G) 24hr Spaced Conditioning memory (PSD-M) performance of $hTau^{0N4R}$-expressing flies kept for 12 days in the ON condition in the absence (0µM) or presence of 10µM MetBlu. $n \geq 11$ per genotype

H) 24hr Spaced Conditioning memory (PSD-M) performance of $hTau^{0N4R}$-expressing flies from the $hTau^{0N4R2a}$ double transgenics, kept for 12 days in the ON condition in the absence (0µM) or presence of 10µM MetBlu. $n \geq 11$ per genotype.

Genotype	Mean ± SEM	F-Ratio	p
Figure 1A.	**ANOVA $F_{(5,74)}$ =17.6036, p=3.34e-11**		
w^{1118}>0N4R (6days)	73.435 ± 2.034		
ElavGal4;$Gal80^{ts}$> w^{1118} (6days)	70.924 ± 2.830	0.5485	0.4614
ElavGal4;$Gal80^{ts}$ >0N4R (6days)	69.789 ± 2.488	1.4645	0.2303
ElavGal4;$Gal80^{ts}$> w^{1118} (6days)	70.924 ± 2.830		
ElavGal4;$Gal80^{ts}$ >0N4R (6days)	69.789 ± 2.488	0.1330	0.7165
w^{1118}>0N4R (12days)	67.671 ± 1.432		
ElavGal4;$Gal80^{ts}$> w^{1118} (12days)	65.831 ± 1.020	0.3580	0.5516
ElavGal4;$Gal80^{ts}$ >0N4R (12days)	50.609 ± 1.981	42.762	**9.00e-9**
ElavGal4;$Gal80^{ts}$> w^{1118} (12days)	65.831 ± 1.020		
ElavGal4;$Gal80^{ts}$ >0N4R (12days)	50.609 ± 1.981	24.507	**5.03e-6**
Figure 1B.	**ANOVA $F_{(5,67)}$=10.433, p=2.7e-7**		
w^{1118}>0N4R (6days)	34.306 ± 3.639		
ElavGal4;$Gal80^{ts}$> w^{1118} (6days)	38.662 ± 3.074	1.1534	0.2870
ElavGal4;$Gal80^{ts}$ >0N4R (6days)	38.128 ± 3.556	0.9688	0.3287
ElavGal4;$Gal80^{ts}$> w^{1118} (6days)	38.662 ± 3.074		
ElavGal4;$Gal80^{ts}$ >0N4R (6days)	38.128 ± 3.556	0.0189	0.8911
w^{1118}>0N4R (12days)	27.931 ± 1.459		
ElavGal4;$Gal80^{ts}$> w^{1118} (12days)	26.506 ± 2.482	0.1418	0.7078
ElavGal4;$Gal80^{ts}$ >0N4R (12days)	16.473 ± 1.656	9.9603	**0.0025**
ElavGal4;$Gal80^{ts}$> w^{1118} (12days)	26.506 ± 2.482		
ElavGal4;$Gal80^{ts}$ >0N4R (12days)	16.473 ± 1.656	7.2917	**0.0089**
Figure 1C.	**ANOVA $F_{(2,40)}$=3.136, p=0.0549**		
w^{1118}>0N4R	65.774 ± 1.955		
ElavGal4;$Gal80^{ts}$> w^{1118}	68.305 ± 1.583	1.053	0.3112
ElavGal4;$Gal80^{ts}$ >0N4R	71.697 ± 1.567	6.179	**0.0174**
ElavGal4;$Gal80^{ts}$> w^{1118}	68.305 ± 1.583		
ElavGal4;$Gal80^{ts}$ >0N4R	71.697 ± 1.567	2.026	0.1628
Figure 1D.	**ANOVA $F_{(2,47)}$=3.202, p=0.0501**		
w^{1118}>0N4R	17.937 ± 1.609		
ElavGal4;$Gal80^{ts}$> w^{1118}	27.051 ± 3.348	5.574	0.0226
ElavGal4;$Gal80^{ts}$ >0N4R	25.300 ± 2.854	3.874	0.0552
ElavGal4;$Gal80^{ts}$> w^{1118}	27.051 ± 3.348		
ElavGal4;$Gal80^{ts}$ >0N4R	25.300 ± 2.854	0.212	0.6477
Figure 1E.	**ANOVA $F_{(3,18)}$ =135.648, p=4.3e-11**		
ElavGal4;$Gal80^{ts}$ >0N4R	1		
ElavGal4;$Gal80^{ts}$ >0N4R^{a1}	0.088 ± 0.0199	272.71	**4.9e-11**
ElavGal4;$Gal80^{ts}$ >0N4R^{a2}	0.0545 ± 0.006	293.05	**2.9e-11**
ElavGal4;$Gal80^{ts}$ >0N4R^{2a}	0.647 ± 0.080	36.188	**2.4e-5**
Figure 1F.	**ANOVA $F_{(2,35)}$ = 143.048, p=5.505e-17**		
w^{1118}>0N4R^{2a}	40.506 ± 1.030		
ElavGal4;$Gal80^{ts}$> w^{1118}	60.492 ± 1.746	119.56	1.65e-12

ElavGal4;Gal80^{ts} >0N4R^{2a}	27.596 ± 1.223	52.768	**2.47e-8**
ElavGal4;Gal80^{ts}> w^{1118}	60.492 ± 1.746		
ElavGal4;Gal80^{ts} >0N4R^{2a}	27.596 ± 1.223	282.78	**9.49e-18**
Figure 1G.	**ANOVA $F_{(2,27)}$=3.119, p=0.062**		
w^{1118}>0N4R^{2a}	66.526 ± 2.471		
ElavGal4;Gal80^{ts}> w^{1118}	72.845 ± 4.099	2.5096	0.1257
ElavGal4;Gal80^{ts} >0N4R^{2a}	62.930 ± 1.753	0.9146	0.3480
ElavGal4;Gal80^{ts}> w^{1118}	72.845 ± 4.099		
ElavGal4;Gal80^{ts} >0N4R^{2a}	62.930 ± 1.753	6.1794	0.0199
Figure 1H.	**ANOVA $F_{(2,42)}$=13.829, p=2.7e-5**		
w^{1118}>0N4R^{2a}	27.926 ± 1.731		
ElavGal4;Gal80^{ts}> w^{1118}	26.202 ± 2.079	0.502	0.4828
ElavGal4;Gal80^{ts} >0N4R^{2a}	16.326 ± 1.246	23.496	**1.9e-5**
ElavGal4;Gal80^{ts}> w^{1118}	26.202 ± 2.079		
ElavGal4;Gal80^{ts} >0N4R^{2a}	16.326 ± 1.246	17.031	**0.0001**
Figure 1I.	**ANOVA $F_{(2,34)}$=2.963, p=0.0659**		
w^{1118}>0N4R^{2a}	20.437 ± 2.228		
ElavGal4;Gal80^{ts}> w^{1118}	25.966 ± 1.669	5.021	0.0321
ElavGal4;Gal80^{ts} >0N4R^{2a}	25.598 ± 1.250	4.375	0.0445
ElavGal4;Gal80^{ts}> w^{1118}	25.966 ± 1.669		
ElavGal4;Gal80^{ts} >0N4R^{2a}	25.598 ± 1.250	0.0272	0.8701
Genotype	**Mean ± SEM**	**Dunnetts' p**	
Figure 2B.	**ANOVA $F_{(1,13)}$=99.548, p=3.7e-7**		
ElavGal4;Gal80^{ts} >0N4R ON	1	1	
ElavGal4;Gal80^{ts} >0N4R OFF	0.544 ± 0.046	**1.1e-8**	
Figure 2C.	**ANOVA $F_{(1,12)}$=1.012, p=0.3327**		
ElavGal4;Gal80^{ts} >0N4R ON	1	1	
ElavGal4;Gal80^{ts} >0N4R OFF	1.205 ± 0.114	0.332	
Figure 2D.	**0N4R: ANOVA $F_{(1,11)}$=0.145, p=0.711** **0N4R^{2a}: ANOVA $F_{(1,13)}$=4.262, p= 0.061**		
ElavGal4;Gal80^{ts} >0N4R ON	1		
ElavGal4;Gal80^{ts} >0N4R OFF	1.009 ± 0.107	0.7114	
ElavGal4;Gal80^{ts} >0N4R^{2a} ON	1		
ElavGal4;Gal80^{ts} >0N4R^{2a} OFF	0.836 ± 0.046	0.0612	
Figure 2E.	**0N4R: ANOVA $F_{(1,11)}$=9.191, p=0.0126** **0N4R^{2a}: ANOVA $F_{(1,9)}$=11.556, p=0.0094**		
ElavGal4;Gal80ts >0N4R ON	1		
ElavGal4;Gal80ts >0N4R OFF	1.656 ± 0.197	**0.0126**	
ElavGal4;Gal80ts >0N4R^{2a} ON	1		
ElavGal4;Gal80ts >0N4R^{2a} OFF	1.879 ± 0.183	**0.0094**	
Genotype	**Mean ± SEM**	**F-Ratio**	**p**
Figure 2F.	**ANOVA $F_{(3,39)}$=12.466, p=9.6e-6**		
w^{1118}>0N4R OFF	30.701 ± 2.261		
ElavGal4;Gal80^{ts}> w^{1118} OFF	41.380 ± 2.698	11.240	0.0019
ElavGal4;Gal80^{ts} >0N4R OFF	32.962 ± 2.346	0.504	0.4825
ElavGal4;Gal80^{ts} >0N4R ON	22.034 ± 1.548	7.405	**0.0099**
ElavGal4;Gal80^{ts}> w^{1118} OFF	41.380 ± 2.698		
ElavGal4;Gal80^{ts} >0N4R OFF	32.962 ± 2.346	6.985	0.0120
ElavGal4;Gal80^{ts} >0N4R ON	22.034 ± 1.548	36.891	**5.5e-7**
ElavGal4;Gal80^{ts} >0N4R OFF	32.962 ± 2.346		
ElavGal4;Gal80^{ts} >0N4R ON	22.034 ± 1.548	11.770	**0.0015**

Figure 2G.	**ANOVA $F_{(3,43)}$ =17.761, p=1.5e-7**		
w^{1118}>0N4R^{2a} OFF	25.398 ± 2.722		
ElavGal4;Gal80^{ts}> w^{1118} OFF	33.028 ± 1.944	7.395	0.009
ElavGal4;Gal80^{ts} >0N4R^{2a} OFF	21.768 ± 0.991	2.061	0.159
ElavGal4;Gal80^{ts} >0N4R^{2a} ON	13.839 ± 1.765	19.541	**7.1e-5**
ElavGal4;Gal80^{ts}> w^{1118} OFF	33.028 ± 1.944		
ElavGal4;Gal80^{ts} >0N4R^{2a} OFF	21.768 ± 0.991	18.625	**9.8e-5**
ElavGal4;Gal80^{ts} >0N4R^{2a} ON	13.839 ± 1.765	50.777	**1.1e-8**
ElavGal4;Gal80^{ts} >0N4R^{2a} OFF	21.768 ± 0.991		
ElavGal4;Gal80^{ts} >0N4R^{2a} ON	13.839 ± 1.765	10.892	**0.002**
Genotype	**Mean ± SEM**	**Dunnetts' p**	
Figure 2H.	**ANOVA $F_{(1,15)}$ =0.018, p=0.8959**		
ElavGal4;Gal80^{ts}> w^{1118} OFF	23.482 ± 1.284	1	
ElavGal4;Gal80^{ts}> w^{1118} ON	23.237 ± 1.308	0.8959	
Genotype	**Mean ± SEM**	**F-Ratio**	**p**
Figure 3C.	**ANOVA $F_{(6,40)}$=0.323, p=0.9204**		
ElavGal4;Gal80^{ts} >0N4R OFF	1		
ElavGal4;Gal80^{ts} >0N4R ON	1.091 ± 0.172	0.128	0.7223
ElavGal4;Gal80^{ts} >0N4R OFF 50µM Met Blu	1.080 ± 0.121	0.0998	0.7539
ElavGal4;Gal80^{ts} >0N4R OFF 100µM Met Blu	0.99345 ± 0.153	0.001	0.9796
ElavGal4;Gal80^{ts} >0N4R OFF 250µM Met Blu	1.245 ± 0.211	0.927	0.3425
ElavGal4;Gal80^{ts} >0N4R OFF 500µM Met Blu	0.952 ± 0.219	0.035	0.8521
ElavGal4;Gal80^{ts} >0N4R OFF 1000µM Met Blu	0.959 ± 0.186	0.023	0.8794
Figure 3D.	**ANOVA $F_{(6,44)}$=4.142, p=0.0027**		
ElavGal4;Gal80^{ts} >0N4R OFF	1		
ElavGal4;Gal80^{ts} >0N4R ON	0.591 ± 0.090	5.1285	0.0293
ElavGal4;Gal80^{ts} >0N4R OFF 50µM Met Blu	0.942 ± 0.118	0.0839	0.7736
ElavGal4;Gal80^{ts} >0N4R OFF 100µM Met Blu	0.822 ± 0.103	0.7924	0.3789
ElavGal4;Gal80^{ts} >0N4R OFF 250µM Met Blu	0.269 ± 0.069	13.301	**0.0008**
ElavGal4;Gal80^{ts} >0N4R OFF 500µM Met Blu	1.034 ± 0.208	0.029	0.864
ElavGal4;Gal80^{ts} >0N4R OFF 1000µM Met Blu	0.892 ± 0.158	0.289	0.593
Genotype	**Mean ± SEM**	**F-Ratio**	**p**
Figure 4A.	**ANOVA $F_{(19,299)}$=1.663 p=0.042**		
ElavGal4;Gal80^{ts}> w^{1118} (2days)	100 ± 0		
ElavGal4;Gal80^{ts}> w^{1118} + 250µM MetBlu (2days)	99.67 ± 0.333	0.245	0.6212
ElavGal4;Gal80^{ts} >0N4R (2days)	99.667 ± 0.333	0.245	0.6212
ElavGal4;Gal80^{ts} >0N4R + 250µM MetBlu (2days)	100 ± 0	2.7e-32	1
ElavGal4;Gal80^{ts}> w^{1118} + 250µM MetBlu (2days)	99.67 ± 0.333		
ElavGal4;Gal80^{ts} >0N4R (2days)	99.667 ± 0.333	2.7e-32	1
ElavGal4;Gal80^{ts} >0N4R + 250µM MetBlu (2days)	100 ± 0	0.245	0.6212

ElavGal4;Gal80^{ts} >0N4R (2days)	99.667 ± 0.333		
ElavGal4;Gal80^{ts} >0N4R + 250µM MetBlu (2days)	100 ± 0	0.245	0.6212
ElavGal4;Gal80^{ts}> w^{1118} (4days)	100 ± 0		
ElavGal4;Gal80^{ts}> w^{1118} + 250µM MetBlu (4days)	99.33 ± 0.454	0.979	0.3233
ElavGal4;Gal80^{ts} >0N4R (4days)	99.33 ± 0.454	0.979	0.3233
ElavGal4;Gal80^{ts} >0N4R + 250µM MetBlu (4days)	100 ± 0	1.1e-31	1
ElavGal4;Gal80^{ts}> w^{1118} + 250µM MetBlu (4days)	99.33 ± 0.454		
ElavGal4;Gal80^{ts} >0N4R (4days)	99.33 ± 0.454	4.2e-34	1
ElavGal4;Gal80^{ts} >0N4R + 250µM MetBlu (4days)	100 ± 0	0.979	0.3233
ElavGal4;Gal80^{ts} >0N4R (4days)	99.33 ± 0.454		
ElavGal4;Gal80^{ts} >0N4R + 250µM MetBlu (4days)	100 ± 0	0.979	0.3233
ElavGal4;Gal80^{ts}> w^{1118} (6days)	100 ± 0		
ElavGal4;Gal80^{ts}> w^{1118} + 250µM MetBlu (6days)	99 ± 0.723	2.203	0.1389
ElavGal4;Gal80^{ts} >0N4R (6days)	99 ± 0.534	2.203	0.1389
ElavGal4;Gal80^{ts} >0N4R + 250µM MetBlu (6days)	100 ± 0	2.4e-31	1
ElavGal4;Gal80^{ts}> w^{1118} + 250µM MetBlu (6days)	99 ± 0.723		
ElavGal4;Gal80^{ts} >0N4R (6days)	99 ± 0.534	6.1e-32	1
ElavGal4;Gal80^{ts} >0N4R + 250µM MetBlu (6days)	100 ± 0	2.203	0.1389
ElavGal4;Gal80^{ts} >0N4R (6days)	99 ± 0.534		
ElavGal4;Gal80^{ts} >0N4R + 250µM MetBlu (6days)	100 ± 0	2.203	0.1389
ElavGal4;Gal80^{ts}> w^{1118} (8days)	100 ± 0		
ElavGal4;Gal80^{ts}> w^{1118} + 250µM MetBlu (8days)	99 ± 0.723	2.203	0.1389
ElavGal4;Gal80^{ts} >0N4R (8days)	98.67 ± 0.766	3.916	0.0488
ElavGal4;Gal80^{ts} >0N4R (8days)	98.67 ± 0.766		
ElavGal4;Gal80^{ts} >0N4R + 250µM MetBlu (8days)	99 ± 0.534	2.203	0.1389
ElavGal4;Gal80^{ts}> w^{1118} + 250µM MetBlu (8days)	99 ± 0.723		
ElavGal4;Gal80^{ts} >0N4R (8days)	98.67 ± 0.766	0.245	0.6212
ElavGal4;Gal80^{ts} >0N4R + 250µM MetBlu (8days)	99 ± 0.534	2.7e-32	1
ElavGal4;Gal80^{ts} >0N4R (8days)	98.67 ± 0.766		
ElavGal4;Gal80^{ts} >0N4R + 250µM MetBlu (8days)	99 ± 0.534	0.245	0.6212
ElavGal4;Gal80^{ts}> w^{1118} (10days)	99.67± 0.333		
ElavGal4;Gal80^{ts}> w^{1118} + 250µM MetBlu (10days)	99 ± 0.723	0.979	0.3233
ElavGal4;Gal80^{ts} >0N4R (10days)	98.33 ± 0.797	3.916	0.0488
ElavGal4;Gal80^{ts} >0N4R + 250µM MetBlu (10days)	98 ± 0.655	6.119	0.01396
ElavGal4;Gal80^{ts}> w^{1118} + 250µM MetBlu (10days)	99 ± 0.723		
ElavGal4;Gal80^{ts} >0N4R (10days)	98.33 ± 0.797	0.979	0.3233

ElavGal4;Gal80^{ts} >0N4R + 250µM MetBlu (10days)	98 ± 0.655	2.203	0.1389
ElavGal4;Gal80^{ts} >0N4R (10days)	98.33 ± 0.797		
ElavGal4;Gal80^{ts} >0N4R + 250µM MetBlu (10days)	98 ± 0.655	0.245	0.6212
Genotype	**Mean ± SEM**	**Dunnetts' p**	
Figure 4B.	**ANOVA $F_{(1,15)}$=0.138, p=0.7154**		
ElavGal4;Gal80^{ts} >0N4R	77.210 ± 1.779	1	
ElavGal4;Gal80^{ts} >0N4R + 250µM MetBlu	78.161 ± 1.834	0.7154	
Figure 4C.	**ANOVA $F_{(1,27)}$=10.435, p=0.0033**		
ElavGal4;Gal80^{ts} >0N4R	34.005 ± 1.815	1	
ElavGal4;Gal80^{ts} >0N4R + 250µM MetBlu	23.804 ± 2.479	**0.0033**	
Figure 4D.	**ANOVA $F_{(1,22)}$=0.201, p=0.6584**		
W^{1118}	42.675 ± 4.298	1	
W^{1118} 250µM MetBlu	40.213 ± 3.297	0.6584	
Figure 4E.	**ANOVA $F_{(1,29)}$ =0.0016, p=0.9681**		
ElavGal4;Gal80^{ts} >0N4R	30.585 ± 1.619	1	
ElavGal4;Gal80^{ts} >0N4R + 250µM MetBlu	30.487 ± 1.817	0.9681	
Figure 4F.	**ANOVA $F_{(1,14)}$=2.056, p=0.1752**		
ElavGal4;Gal80^{ts} >0N4R	30.584 ± 3.218	1	
ElavGal4;Gal80^{ts} >0N4R + 500µM MetBlu	37.413 ± 3.521	0.1752	
Figure 4G.	**ANOVA $F_{(1,23)}$=0.701, p=0.4115**		
W^{1118}	26.104 ± 2.944	1	
W^{1118} 500µM MetBlu	30.460 ± 4.290	0.4115	
Genotype	**Mean ± SEM**	**F-Ratio**	**p**
Figure 5A.	**ANOVA $F_{(1,9)}$=51.036, p=9.8e-5**		
ElavGal4;Gal80^{ts} >0N4R	1	1	
ElavGal4;Gal80^{ts} >0N3R	6.049 ± 0.516	**7.7e-5**	
Figure 5B.	**Soluble: ANOVA $F_{(3,15)}$=0.495, p=0.6927** **Insoluble: ANOVA $F_{(3,48)}$ =3.013, p=0.0397**		
Soluble			
ElavGal4;Gal80^{ts} >0N3R	1		
ElavGal4;Gal80^{ts} >0N3R 10µM Met Blu	1.042 ± 0.154	0.0377	0.8492
ElavGal4;Gal80^{ts} >0N3R 50µM Met Blu	1.071 ± 0.146	0.107	0.7495
ElavGal4;Gal80^{ts} >0N3R 100µM Met Blu	1.246 ± 0.159	1.280	0.2799
Insoluble			
ElavGal4;Gal80^{ts} >0N3R	1		
ElavGal4;Gal80^{ts} >0N3R 10µM Met Blu	0.816 ± 0.115	1.704	0.1984
ElavGal4;Gal80^{ts} >0N3R 50µM Met Blu	0.578 ± 0.058	8.970	**0.0044**
ElavGal4;Gal80^{ts} >0N3R 100µM Met Blu	0.782 ± 0.133	2.484	0.1219
Genotype	**Mean ± SEM**	**F-Ratio**	**p**
Figure 5C.	**ANOVA $F_{(23,407)}$=8.534, p=5.1e-23**		
ElavGal4;Gal80^{ts}> w^{1118} (2days)	96.765 ± 0.851		
ElavGal4;Gal80^{ts}> w^{1118} + 50µM MetBlu (2days)	97.353 ± 1.060	0.055	0.8154

ElavGal4;Gal80^{ts} >0N3R (2days)	98.529 ± 0.713	0.491	0.4839
ElavGal4;Gal80^{ts} >0N3R + 50µM MetBlu (2days)	98.235 ± 0.597	0.341	0.5596
ElavGal4;Gal80^{ts}> w^{1118} + 50µM MetBlu (2days)	97.353 ± 1.060		
ElavGal4;Gal80^{ts} >0N3R (2days)	98.529 ± 0.713	0.218	0.6406
ElavGal4;Gal80^{ts} >0N3R + 50µM MetBlu (2days)	98.235 ± 0.597	0.123	0.7262
ElavGal4;Gal80^{ts} >0N3R (2days)	98.529 ± 0.713		
ElavGal4;Gal80^{ts} >0N3R + 50µM MetBlu (2days)	98.235 ± 0.597	0.014	0.9071
ElavGal4;Gal80^{ts}> w^{1118} (4days)	95 ± 1.213		
ElavGal4;Gal80^{ts}> w^{1118} + 50µM MetBlu (4days)	96.471 ± 1.407	0.341	0.5596
ElavGal4;Gal80^{ts} >0N3R (4days)	93.529 ± 1.647	0.341	0.5596
ElavGal4;Gal80^{ts} >0N3R + 50µM MetBlu (4days)	94.706 ± 1.740	0.014	0.9071
ElavGal4;Gal80^{ts}> w^{1118} + 50µM MetBlu (4days)	96.471 ± 1.407		
ElavGal4;Gal80^{ts} >0N3R (4days)	93.529 ± 1.647	1.364	0.2436
ElavGal4;Gal80^{ts} >0N3R + 50µM MetBlu (4days)	94.706 ± 1.740	0.491	0.4839
ElavGal4;Gal80^{ts} >0N3R (4days)	93.529 ± 1.647		
ElavGal4;Gal80^{ts} >0N3R + 50µM MetBlu (4days)	94.706 ± 1.740	0.218	0.6406
ElavGal4;Gal80^{ts}> w^{1118} (6days)	93.529 ± 1.532		
ElavGal4;Gal80^{ts}> w^{1118} + 50µM MetBlu (6days)	94.118 ± 1.5597	0.055	0.8154
ElavGal4;Gal80^{ts} >0N3R (6days)	89.412 ± 1.813	2.673	0.1028
ElavGal4;Gal80^{ts} >0N3R + 50µM MetBlu (6days)	88.529 ±1.807	3.942	**0.0478**
ElavGal4;Gal80^{ts}> w^{1118} + 50µM MetBlu (6days)	94.118 ± 1.5597		
ElavGal4;Gal80^{ts} >0N3R (6days)	89.412 ± 1.813	3.492	0.0624
ElavGal4;Gal80^{ts} >0N3R + 50µM MetBlu (6days)	88.529 ±1.807	4.924	**0.0271**
ElavGal4;Gal80^{ts} >0N3R (6days)	89.412 ± 1.813		
ElavGal4;Gal80^{ts} >0N3R + 50µM MetBlu (6days)	88.529 ±1.807	0.123	0.7262
ElavGal4;Gal80^{ts}> w^{1118} (8days)	91.471 ± 1.471		
ElavGal4;Gal80^{ts}> w^{1118} + 50µM MetBlu (8days)	92.941 ± 1.549	0.341	0.5596
ElavGal4;Gal80^{ts} >0N3R (8days)	87.353 ± 1.923	2.673	0.1028
ElavGal4;Gal80^{ts} >0N3R + 50µM MetBlu (8days)	83.529 ± 2.804	9.944	**0.0017**
ElavGal4;Gal80^{ts}> w^{1118} + 50µM MetBlu (8days)	92.941 ± 1.549		
ElavGal4;Gal80^{ts} >0N3R (8days)	87.353 ± 1.923	4.924	**0.0271**
ElavGal4;Gal80^{ts} >0N3R + 50µM MetBlu (8days)	83.529 ± 2.804	13.968	**0.0002**
ElavGal4;Gal80^{ts} >0N3R (8days)	87.353 ± 1.923		
ElavGal4;Gal80^{ts} >0N3R + 50µM MetBlu (8days)	83.529 ± 2.804	2.305	0.1298
ElavGal4;Gal80^{ts}> w^{1118} (10days)	90.882 ± 1.5597		
ElavGal4;Gal80^{ts}> w^{1118}	91.176 ± 1.518	0.014	0.9071

+ 50µM MetBlu (10days)			
ElavGal4;Gal80^{ts} >0N3R (10days)	86.176 ± 2.123	3.492	0.0624
ElavGal4;Gal80^{ts} >0N3R + 50µM MetBlu (10days)	82.059 ± 2.910	12.276	**0.0005**
ElavGal4;Gal80^{ts}> w^{1118} + 50µM MetBlu (10days)	91.176 ± 1.518		
ElavGal4;Gal80^{ts} >0N3R (10days)	86.176 ± 2.123	3.942	**0.0478**
ElavGal4;Gal80^{ts} >0N3R + 50µM MetBlu (10days)	82.059 ± 2.910	13.108	**0.0003**
ElavGal4;Gal80^{ts} >0N3R (10days)	86.176 ± 2.123		
ElavGal4;Gal80^{ts} >0N3R + 50µM MetBlu (10days)	82.059 ± 2.910	2.673	0.1028
ElavGal4;Gal80^{ts}> w^{1118} (12days)	89.412 ± 1.813		
ElavGal4;Gal80^{ts}> w^{1118} + 50µM MetBlu (12days)	91.176 ± 1.518	0.491	0.4839
ElavGal4;Gal80^{ts} >0N3R (12days)	85.588 ± 2.095	2.305	0.1298
ElavGal4;Gal80^{ts} >0N3R + 50µM MetBlu (12days)	79.118 ± 3.008	16.709	**5.3e-5**
ElavGal4;Gal80^{ts}> w^{1118} + 50µM MetBlu (12days)	91.176 ± 1.518		
ElavGal4;Gal80^{ts} >0N3R (12days)	85.588 ± 2.095	4.924	**0.0271**
ElavGal4;Gal80^{ts} >0N3R + 50µM MetBlu (12days)	79.118 ± 3.008	22.929	**2.4e-6**
ElavGal4;Gal80^{ts} >0N3R (12days)	85.588 ± 2.095		
ElavGal4;Gal80^{ts} >0N3R + 50µM MetBlu (12days)	79.118 ± 3.008	6.602	**0.0106**
Genotype	**Mean ± SEM**	**Dunnetts' p**	
Figure 5D.	**ANOVA $F_{(1,23)}$=0.107, p=0.7470**		
ElavGal4;Gal80^{ts} >0N3R	61.532 ± 2.408	1	
ElavGal4;Gal80^{ts} >0N3R + 50µM MetBlu	62.742 ± 2.815	0.7470	
Figure 5E.	**ANOVA $F_{(1,28)}$=9.407, p=0.0049**		
ElavGal4;Gal80^{ts} >0N3R	33.772 ± 2.136	1	
ElavGal4;Gal80^{ts} >0N3R + 50µM MetBlu	24.232 ± 2.201	**0.0049**	
Figure 5F.	**ANOVA $F_{(1,20)}$=4.120, p=0.0566**		
ElavGal4;Gal80^{ts} >0N3R	30.408 ± 3.872	1	
ElavGal4;Gal80^{ts} >0N3R + 50µM MetBlu	36.975 ± 2.589	0.0566	
Figure 5G.	**ANOVA $F_{(1,28)}$=0.113, p=0.7397**		
W^{1118}	23.995 ± 2.303	1	
W^{1118} + 50µM MetBlu	22.931 ± 2.180	0.7397	
Figure 5H.	**ANOVA $F_{(1,25)}$ =0.007, p=0.936**		
ElavGal4;Gal80^{ts} >0N3R	34.074 ± 4.120	1	
ElavGal4;Gal80^{ts} >0N3R + 10µM MetBlu	34.520 ± 3.649	0.936	
Figure 5I.	**ANOVA $F_{(1,23)}$=0.571, p=0.458**		
ElavGal4;Gal80^{ts} >0N3R	39.685 ± 2.389	1	
ElavGal4;Gal80^{ts} >0N3R + 100µM MetBlu	37.081 ± 2.485	0.458	
Figure 5J.	**ANOVA $F_{(1,23)}$=7.211, p=0.0135**		
ElavGal4;Gal80^{ts} >0N4R	24.318 ± 3.448	1	
ElavGal4;Gal80^{ts} >0N4R + 50µM MetBlu	12.492 ± 2.739	**0.0135**	
Figure 5K.	**ANOVA $F_{(1,22)}$=2.576, p=0.1234**		

ElavGal4;Gal80^{ts} >0N4R	27.778 ± 2.615	1	
ElavGal4;Gal80^{ts} >0N4R + 100µM MetBlu	22.875 ± 1.420	0.1234	
Genotype	**Mean ± SEM**	**Dunnetts' p**	
Figure 7A.	**ANOVA $F_{(1,11)}$=37.416, p=0.0001**		
ElavGal4;Gal80^{ts} >0N4R	1	1	
LeoGal4;Gal80^{ts} >0N4R	14.199 ± 1.586	**0.0001**	
Figure 7B.	**ANOVA $F_{(1,11)}$=34.926, p= 0.0001**		
ElavGal4;Gal80^{ts} >0N4R^{2a}	1	1	
LeoGal4;Gal80^{ts} >0N4R^{2a}	4.341 ± 0.671	**0.0001**	
Genotype	**Mean ± SEM**	**F-Ratio**	**p**
Figure 7C.	**ANOVA $F_{(2,39)}$=1.527, p=0.2306**		
LeoGal4;Gal80^{ts} >W^{1118}	37.573 ± 3.367		
W^{1118} > 0N4R	31.291 ± 2.029	2.308	0.1372
LeoGal4;Gal80^{ts} >0N4R	31.915 ± 2.564	2.201	0.1463
W^{1118} > 0N4R	31.291 ± 2.029		
LeoGal4;Gal80^{ts} >0N4R	31.915 ± 2.564	0.0234	0.8792
Figure 7D.	**ANOVA $F_{(2,39)}$=2.706, p=0.0799**		
LeoGal4;Gal80^{ts} >W^{1118}	35.773 ± 3.475		
W^{1118} > 0N4R^{2a}	29.079 ± 2.046	3.2223	0.0808
LeoGal4;Gal80^{ts} >0N4R^{2a}	27.518 ± 2.306	4.9009	0.0331
W^{1118} > 0N4R^{2a}	29.079 ± 2.046		
LeoGal4;Gal80^{ts} >0N4R^{2a}	27.518 ± 2.306	0.1899	0.6655
Genotype	**Mean ± SEM**	**Dunnetts' p**	
Figure 7E.	**Soluble: ANOVA $F_{(1,11)}$= 291.294, p=1.0e-8** **Insoluble: ANOVA $F_{(1,11)}$=49.499, p=3.6e-5**		
Soluble			
ElavGal4;Gal80^{ts} >0N4R	1	1	
LeoGal4;Gal80^{ts} >0N4R	5.256 ± 0.249	**6.9e-10**	
Insoluble			
ElavGal4;Gal80^{ts} >0N4R	1	1	
LeoGal4;Gal80^{ts} >0N4R	4.445 ± 0.447	**3.1e-5**	
Figure 7F.	**ANOVA $F_{(1,23)}$=0.719, p=0.4797**		
LeoGal4;Gal80^{ts} >0N4R	72.327 ± 2.333	1	
LeoGal4;Gal80^{ts} >0N4R + 10µM MetBlu	69.959 ± 2.324	0.4797	
Figure 7G.	**ANOVA $F_{(1,23)}$=6.768, p=0.0163**		
LeoGal4;Gal80^{ts} >0N4R	37.588 ± 3.709	1	
LeoGal4;Gal80^{ts} >0N4R + 10µM MetBlu	26.842 ± 1.816	**0.0163**	
Figure 7H.	**ANOVA $F_{(1,23)}$=6.192, p=0.0209**		
LeoGal4;Gal80^{ts} >0N4R^{2a}	40.723 ± 2.455	1	
LeoGal4;Gal80^{ts} >0N4R^{2a} + 10µM MetBlu	30.747 ± 3.169	**0.0209**	

Table 4. Collective statistics Table.

The means and SEMs for Immediate Memories (Learning) PSD-M and PSI-M performance and viabilities (Fig 4A and 5C), of the indicated genotypes are shown. Following the indicated ANOVA the means were compared using planned multiple comparisons. Significant differences are highlighted in bold.